SIZES AND INTENSITIES OF MESOSCALE PRECIPITATION AREAS AS DEPICTED BY DIGITAL RADAR DATA

by

LARRY EUGENE FREEMAN

B. S., Mississippi State University
(1971)

B.S., Oklahoma University
(1972)

SUBMITTED IN PARTIAL FULFILLMENT

OF THE REQUIREMENTS FOR THE

DEGREE OF MASTER OF SCIENCE

at the

MASSACHUSETTS INSTITUTE OF
TECHNOLOGY

January, 1976

Signature of Author .....
Department of Meteorology, January 21, 1976

Certified by .....
Thesis Supervisor

Accepted by .....
Chairman, Departmental Committee
on Graduate Students

SIZES AND INTENSITIES OF MESOSCALE PRECIPITATION AREAS
AS DEPICTED BY DIGITAL RADAR DATA

by

LARRY EUGENE FREEMAN

Submitted to the Department of Meteorology on January 21, 1976
in partial fulfillment of the requirements for
the degree of Master of Science

ABSTRACT

A study of mesoscale precipitation areas in five storms was undertaken using a digital radar data base. A FORTRAN computer program was developed which accepts digital radar maps in polar coordinates and determines the area-weighted centroids and sizes of precipitation areas defined by a given intensity threshold. The output from this program was analyzed to determine intensity thresholds which could be used to define the large and small mesoscale precipitation areas which had been observed in earlier studies. Also, characteristics of the precipitation areas which could be used in modeling were sought.

The shape of the curves showing the number of separate areas as a function of intensity and a parameter which involved both the number and size of the areas indicated that intensity thresholds in the vicinity of 30 dbz and 36-38 dbZ were ones at which significant merging of several areas into one occurred. Therefore, these thresholds were identified as suitable ones to define large mesoscale areas and small mesoscale areas. Although there were a large number of areas at each intensity threshold, the larger more important areas defined by these threshold regions were found to be of acceptable size to lend support to the contention that they could define large and small mesoscale areas.

The distribution of areal coverage with intensity was found to be very well behaved for entire maps as well as for individual precipitation areas. In general, for individual areas the fourth root of areal coverage was found to vary linearly with the increment in intensity above the threshold used to define the area. Empirical relations were obtained to predict the distribution of area with intensity for areas defined by the 24 dbZ threshold in terms of their size for a squall line and a cyclonic storm. A strong relationship was observed between the size of areas and the peak intensity of the areas which permitted the determination of empirical relations to predict the size of areas at various intensity thresholds in terms of the peak intensity of the areas for a squall line and a cyclonic storm. Possible applications of these empirical relations to modeling are considered and a discussion of various criteria to separate significant precipitation areas from insignificant ones is provided.

Thesis Supervisor: Pauline M. Austin
Title: Senior Research Associate

TABLE OF CONTENTS

LIST OF TABLES

LIST OF FIGURES

LIST OF FIGURES (continued)

page

I. INTRODUCTION

A. THE OVERVIEW

In the past several years there has been considerable interest in the scale of atmospheric phenomena which lies between the large-scale synoptic features and the small-scale cellular activity. One way in which mesoscale phenomena have been investigated is through the study of rain patterns associated with large scale systems. Such studies have been undertaken mainly through the use of weather radar since radar seems to offer the only convenient means of observing this intermediate scale of meteorological activity. Most of the data for these studies were Plan Position Indicator (PPI) displays which were recorded on 35-mm film at time intervals of a few minutes so as to yield a more or less continuous picture of activity in a storm. These displays often depicted signals which had been quantized into intensity levels. Although these displays were more meaningful than unquantized ones, a great deal of fine structure could still be missed within a given intensity level since there were often 5-10 db between intensity levels. More recently, with the advent of digital radar data, these intensity gaps can be filled in.

To date much of the work using digital radar data has been concerned with the problems of data handling. Several recent reports describe various techniques which have been developed for application to digital radar data (Blackmer and Duda, 1972; Wiggert and Andrews, 1974). These have dealt mainly with solutions to hardware problems although some effort has been devoted to the problems of pattern

recognition and analysis using digital radar data bases. Most of the analysis has been in the form of computer software capable of determining rainfall amounts within given echoes, and tracking echoes (Blackmer and Duda, 1972; Ostlund, 1974). Little attention has been paid to the problem of analyzing individual precipitation areas as entities in themselves. Indeed, the usefulness of techniques to track echoes cannot be denied. However, mesoscale precipitation areas often appear not as isolated entities but as part of a complex pattern in a region of widespread rain. Therefore, prior to tracking echoes, it is necessary to have an understanding of the characteristics and behavior of precipitation areas in order to determine which echoes are of enough significance to track. Echoes of enough significance to track would be those echoes which could be described as mesoscale precipitation areas. Therefore, a study using digital radar data to attempt to describe mesoscale precipitation areas and to determine their boundaries when they are embedded in lighter precipitation would seem to be in order.

B. BACKGROUND

A great deal of organization has been observed in precipitation patterns and documented in the literature. Austin (1960) reported banded structures some 80-100 kilometers wide and 460 kilometers long across the warm frontal areas in two New England storms. Elliott and Hovind (1964) undertook a study of four storms on the California coast. They observed that each storm contained precipitation bands

that were 40-80 kilometers wide and separated by 60-120 kilometers. These bands contained all the cells observable in the storms and maintained their identities for periods of up to 3 hours. Browning and Harrold (1969) found banded structures ahead of the warm front and in the warm sector of one cyclone in England. Austin and Houze (1972) observed that of seventeen New England cyclones which they studied all contained banded structures. Almost all the investigators noted that the banded structures contained smaller scale phenomena.

Austin and Houze (1972) and Reed (1972) undertook studies of these smaller entities. Austin and Houze divided these smaller precipitation areas into large mesoscale areas (LMSA's) and small mesoscale areas (SMSA's) with each being defined in terms of size and duration. The SMSA's were generally defined as being less than $10^3 km^2$ in areal coverage with lifetimes on the order of one hour. The LMSA's were larger than $10^3 km^2$ with lifetimes of several hours. Reed (1972) undertook a study of the larger mesoscale precipitation areas in eight New England cyclones. He found three distinct types of banded structures based on size and shape. These bands and associated LMSA's accounted for virtually all of the heavy rainfall in the storms.

C. THE PROBLEM

Although there has been considerable evidence presented in the past for the existence of mesoscale precipitation areas, precise methods of identification and detailed characteristics of this intermediate scale phenomenon have not been determined. Because

digital radar data offers a much higher degree of resolution than the photographic data, it will reveal far more detail on the fine structure of mesoscale precipitation areas. Computer techniques must be developed to analyze the digital data and therefore a need exists for definitions and techniques to identify the mesoscale precipitation areas. The purpose of this study will be to use a digital radar data base to seek identification techniques for mesoscale areas and to determine characteristics of precipitation areas in terms of size and intensity.

II. THE DATA BASE

A. THE DIGITAL MAPS

The data used for this study was in the form of digital radar maps taken by the WR66 and WR73 weather radars that are operated by the Department of Meteorology at the Massachusetts Institute of Technology. The characteristics of these radars are given in Table 1. The digital maps are stored on magnetic Dectapes by a PDP-8I minicomputer which accepts signals directly from both radars. Resolution in the data is 1° in azimuth and 100 bins in range with the range increment being determined by the range of the map (i.e., 1/2 nautical mile for a 50 nautical mile range; 1 n.m. for a 100 n.m. range; and 2 n.m. for a 200 n.m. range). An input parameter is supplied when recording a map to indicate how many range bins should be skipped before data are recorded. Since this is an input variable, the initial range varies from map to map.

The digital maps are stored and used in dbZ* units with hard-copies of the map being displayed in B-SCAN format. The B-SCAN format was chosen because it is the most convenient method of examining the data although rather gross distortion of shapes results. The B-SCAN format takes data in r,θ coordinates and treats it as if it were rectangular with x being r and y being θ. The result is that data at close ranges appears to be spread in the azimuthal direction and data

---

*Reflectivity is expressed in dbZ units with dbZ defined by dbZ = 10 log Z where Z is equivalent reflectivity factor in $mm^6 m^{-3}$.

Table 1. Characteristics of the WR66 and WR73 radars

Parameter	WR66	WR73
Wavelength (cm)	10.5	5.5
Beam Width (half power points in deg)	1.35	1.40
Pulse Length (μsec)	1.0	2.0
Nominal Transmitted Power (kw)	600	250
Frequency (MHz)	2850	5550

at far ranges appears to be compacted. An example of a section of a digital map displayed in B-SCAN is shown in Figure 1.

B. PROBLEMS WITH THE DATA

Because of the limited capacity of the PDP-8 computer, most of the analysis of the data had to be accomplished on the IBM 370 computer at the Massachusetts Institute of Technology Information Processing Center. Consequently, the data had to be transferred from the small PDP-8 Dectapes to a form useable by the IBM machine. The method chosen was to punch the digital maps to paper tape on the PDP-8; transfer the paper tape to the IPC; and translate the paper tape to cards for input to the IBM machine. Although the method was time consuming, it allowed for all the quality control to be done before the data was input to the IBM machine.

Another problem encountered with the data was the presence of ground clutter. This problem is inherent in nearly all radar systems although it is enhanced at MIT because of the location in a large metropolitan area with relatively large hills in the surrounding regions. At low elevation angles permanent echoes cover most of the area out to about 37 kilometers (20 n.m.). Techniques for eliminating

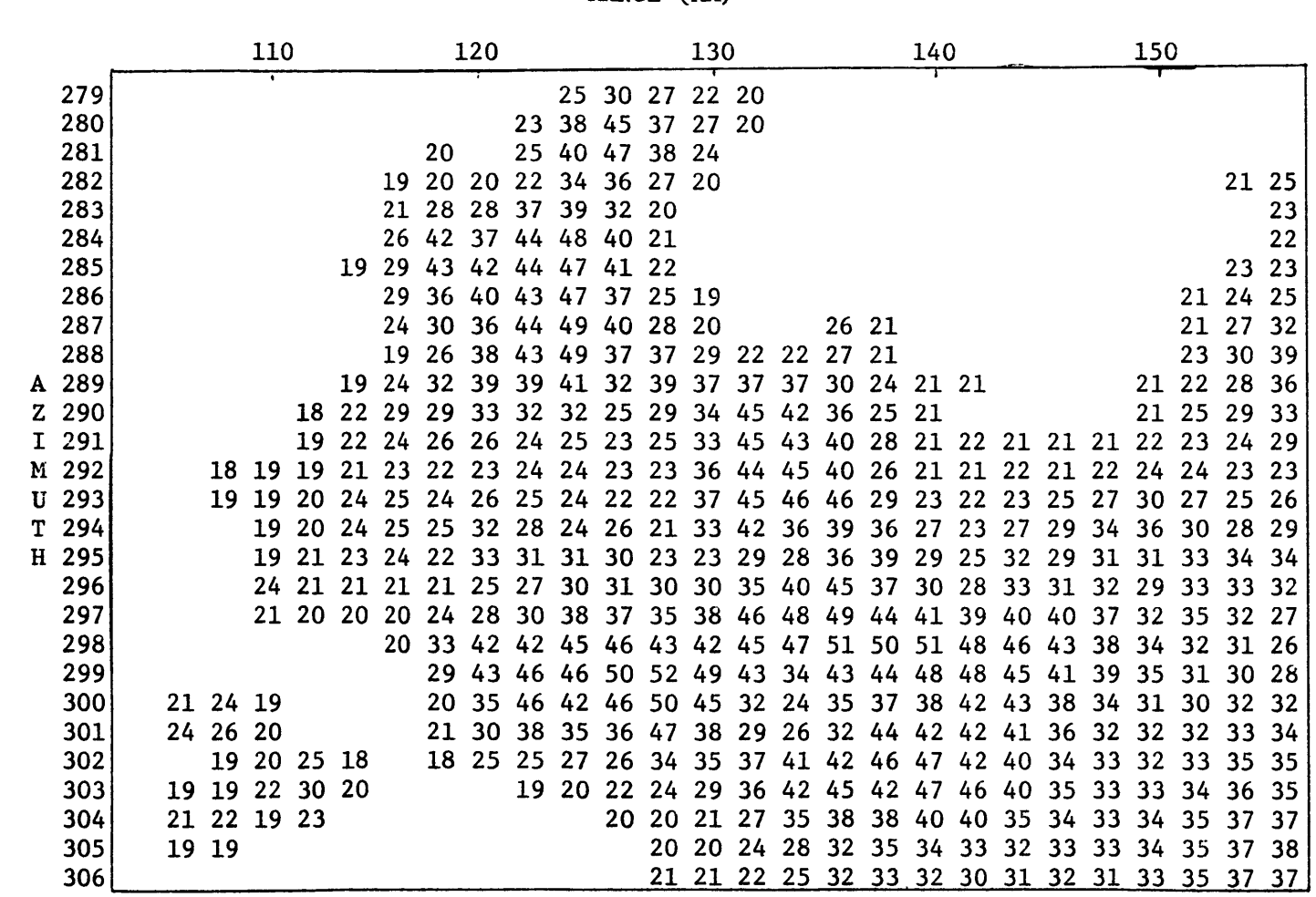

Figure 1. Section of digital map 4f in B-SCAN format showing reflectivity factor in dbZ

such ground targets have been suggested by Johnson, Smith, Nathanson and Brooks (1975) and Schaffner (1975). The most promising techniques appear to be echo processing ones based upon measurement of the rate of echo fluctuation and echo fluctuation magnitude. Research is currently underway to make such techniques operational. Meanwhile, the approach taken in this study was simply to start the analysis at 37 kilometers (20 n.m.) with the assumption that nearly all ground clutter effects are within 37 km.

Several prominent echoes occur as a result of mountains well beyond 37 km in range. The problem which they pose is relatively easy to solve when there is no precipitation occurring directly over the mountains. When this is the case, the ground targets can be manually removed from the maps because the targets occur in the same position on every map. However, if the mountains are enclosed by precipitation, then it becomes more difficult to determine the effect of the ground targets. In general, when the targets are surrounded by precipitation one can observe an enhancement of the signal in the position where the ground targets are known to occur. However, whether this enhancement is a result of intensification of the precipitation caused by the mountains or a result of the mountains themselves is difficult if not impossible to determine. The procedure used in this study was to completely remove the ground targets manually whenever possible (i.e. when no precipitation was occurring directly over the mountains). When the targets were surrounded by precipitation, the assumption was that the enhancement of signal was caused by the mountains themselves, and

the peaks in the vicinity of the ground targets were removed from the data down to the point where it became impossible to distinguish the ground targets from the surrounding precipitation.

Another effect not within 37km occurs in the case of shadows caused by ground targets such as tall buildings at very close range. These shadows would have a drastic effect on statistics of size distributions of precipitation areas. They essentially are capable of dividing one continuous area into two areas. Since most of the shadows caused by ground targets are in the sector between 90° and 160° azimuth for the radar systems at MIT, this sector was avoided as much as possible.

C. THE STORMS CHOSEN FOR STUDY

The storms selected for study were chosen not only on the basis of the storm type and characteristics but also on the avialability of data. Digital maps have been taken at MIT since the fall of 1974 but with very limited coverage until the summer of 1975. The number of digital maps available was, therefore, quite limited and this was the most important consideration. At least one storm was chosen in each season of the year with extensive case histories done on a summertime squall line and a fall storm. Table 2 gives the pertinent characteristics of the maps for each storm. In a complete map sequence, the radar scans at a series of elevation angles providing three dimensional coverage. The low elevation angle maps were chosen for all storms considered.

Table 2. Characteristics of the maps for each storm

Map	Date	Time (EST)	Radar	Range (km)	Azimuth	Elevation (deg)
1	20 Sep 74	1532	WR66	185	260-020	.6
2	16 Dec 74	1655	WR66	92.5	165-330	.7
3	3 Apr 75	1635	WR73	92.5	290-130	.8
4a	9 Jul 75	1308	WR66	185	250-010	.7
4b	9 Jul 75	1320	WR66	185	250-010	.7
4c	9 Jul 75	1345	WR66	185	245-010	.7
4d	9 Jul 75	1405	WR66	185	245-010	.7
4e	9 Jul 75	1430	WR66	185	245-010	.7
4f	9 Jul 75	1500	WR66	185	245-010	.7
4g	9 Jul 75	1545	WR66	185	245-020	.7
4h	9 Jul 75	1624	WR66	185	245-020	.7
4i	9 Jul 75	1640	WR66	185	245-020	.7
4j	9 Jul 75	1700	WR66	185	245-020	.7
4k	9 Jul 75	1730	WR66	185	245-020	.7
4l	9 Jul 75	1750	WR66	185	245-020	.7
4m	9 Jul 75	1811	WR66	185	230-025	.7
4n	9 Jul 75	1827	WR66	185	230-030	.7
4o	9 Jul 75	1840	WR66	185	230-030	.7
5a	24 Sep 75	0932	WR66	185	225-045	.5
5b	24 Sep 75	0944	WR66	185	225-045	.5
5c	24 Sep 75	0952	WR66	185	225-045	.5
5d	24 Sep 75	1006	WR66	185	225-045	.5
5e	24 Sep 75	1017	WR66	185	225-030	.5
5f	24 Sep 75	1031	WR66	185	225-030	.5

For the first three storms only single maps were available. Therefore, time variations could not be considered. The storm of September 20, 1974, was a fall squall line of rather weak intensity. The winter storm of December 16, 1974, was a cyclonic storm characterized by widespread rain and a large range of intensity. The springtime case, April 3, 1975, again was a cyclonic storm with widespread rain but exhibited a smaller intensity range than the December case.

The squall line of July 9, 1975, was an intense storm with a large range of intensity. The storm formed a line from several patches of precipitation and moved steadily toward Boston from the west for the 5 1/2 hours it was observed by the radar. The intensity of the storm seemed to remain fairly constant after the line had formed. However, the line appeared to be weakening near the end of the observation period (≈1800E). The storm was a classic summertime squall line which formed in early afternoon and began dying near sunset.

The storm of September 24, 1975, was more cyclonic in character although it did exhibit some characteristics of a line. The intensity range was not great during the early observation period with the precipitation being mostly widespread light rain. However, the storm showed signs of intensification toward the end of the observation period. In general, this was a cyclonic storm characteristic of fall cyclones in New England.

III. METHODS OF ANALYSIS

A. THE CENTROID PROGRAM

The basic tool of analysis for this study was a computer program written in FORTRAN which was capable of identifying precipitation areas at a given intensity threshold and outputting the areal coverage, and the area-weighted centroid in r,θ coordinates as defined by:

$$\bar{r} = \frac{\sum r_i A_i}{\sum A_i} \qquad \text{and} \qquad \bar{\theta} = \frac{\sum \theta_i A_i}{\sum A_i}$$

The input to the program was a digital map in r,θ coordinates, the initial range and the total range of the map. The program then output a hard copy of the digital map in B-SCAN format and generated a range array and an area array each consisting of 100 elements corresponding to the range and the area associated with each data point. Any data point within 20 n.m. (37km) of the radar was eliminated as ground clutter and the map was then searched for the maximum intensity value it contained. The program then began execution of the complex logic to locate separate areas and compute their centroids.

Each azimuth ray was composed of 100 data points in bin numbers 1-100. In the program each azimuth was searched for dbZ values in excess of a given threshold value and the beginning and ending bin numbers for strings of data points exceeding the threshold were stored in pointer arrays. Next, the azimuths were considered two at a time to find continuous areas in excess of the threshold. Continuous areas

would be those which exceeded the threshold value at the same bin numbers within 1 on two consecutive azimuths. When these matching precipitation areas were found, the sums of (1) the areal coverage, (2) the product of the area and range, and (3) the product of the area and azimuth were determined for each bin in each separate precipitation area and these sums were maintained in appropriate arrays. Each precipitation area was identified by a number and the bin numbers which it included along each azimuth were maintained in other pointer arrays. Logical steps were then performed to merge overlapping areas into one area for identification purposes. Before incrementing in azimuth to make these same comparisons between the second azimuth under consideration and the next azimuth on the map, the first azimuth was checked to detect areas which were detectable on only one azimuth.

An illustrative example may help to clarify the procedure. Consider a simple map of 5 azimuths and 10 range bins as shown in Figure 2. The bins marked with an X are in excess of the threshold intensity value. First the beginning and ending bin numbers for excess values would be determined for each azimuth. For azimuth number 2, the first beginning point would be bin number 1 and the corresponding ending point would be bin number 3. The second beginning point is bin number 8 with its corresponding ending point being bin number 9. This procedure is accomplished for each azimuth. The azimuths are then considered two at a time. Using azimuths 1 and 2, the program would match the first excess area on azimuth 1, namely bin number 2, with the first excess area on azimuth number 2 which runs from bin

BIN NUMBER

AZIMUTH	1	2	3	4	5	6	7	8	9	10
1		X				X			X	
2	X	X	X					X	X	
3		X	X	X			X	X	X	
4		X	X	X	X		X	X	X	X
5				X	X	X	X	X		

Figure 2. Simplified digital map to illustrate program logic

number 1 to bin number 3. This match would cause identification number 1 to be assigned to this area and the three sums for area number 1 would be computed and stored. A similar match would occur for bin number 9 on azimuth 1 and bin numbers 8-9 on azimuth 2. This would lead to the same sums being computed and stored for an area identified as area number 2. Before moving on to consider azimuths 2 and 3 together, the program would search azimuth 1 for any excess bin numbers which had not been included in any sums made. Consequently, bin number 6 would be discovered and assigned area number 3. When azimuths 2 and 3 were considered together, bin numbers 2-4 on azimuth 3 would be summed to area 1 and bin numbers 7-9 would be summed to area 2. No further contribution would be made to area 3 since it was not a continuous area. The consideration of azimuths 3 and 4 would result in the additions of the appropriate bin numbers on azimuth 4 to the areas identified as numbers 1 and 2. However, when azimuths 4 and 5 were considered, the two separate areas would be merged ot one. The

first match would allow bin numbers 4-8 on azimuth 5 to be added to area number 1. Logical steps were included in the program which allowed the same bin numbers on each azimuth to be used only once. Therefore, when a match occurred between bin numbers 4-8 on azimuth 5 and bin numbers 7-10 on azimuth 4 (which correspond to area number 2), no sums would be made. Instead, during the search for overlapping areas, the sums associated with area number 2 would be transferred and added to the appropriate sums for area number 1 and area number 2 would cease to exist. The two areas identified on this simple map would be area number 1 and area number 3.

B. ANALYSIS TECHNIQUES APPLIED TO OUTPUT

When these steps were performed over the entire map, the program would output the identification number of the precipitation area, the total area covered, and the area-weighted centroid in r,θ coordinates. Also output was the total area covered by precipitation in excess of the threshold intensity over the entire map, the average size of the areas identified at that intensity, and the size of the largest area identified. The threshold was then reduced by 2 dbZ and the entire process was repeated for this new threshold value. The program started at the maximum intensity on the map and terminated at the 20 dbZ threshold. A copy of the FORTRAN program is provided in Appendix I.

Several analyses were performed on the output from the centroid program in an attempt to find thresholds which would define mesoscale areas as well as to determine characteristics of areas which could be

used in the development of storm models. For each map, the distribution of total areal coverage, number of areas and sizes of identified areas were determined as a function of intensity threshold. Another technique employed consisted of matching each area at a given threshold value to the area it was associated with at the next lower threshold value. This allowed for the determination of rates of decrease in areal coverage with increasing intensity in individual precipitation areas as well as in the storm as a whole. Relations were sought between the size of the areas identified at some threshold intensity value and the peak intensity which they contained. The threshold intensity value is also referred to as the base contour level. It is simply the intensity threshold being used to identify the precipitation areas under consideration.

IV. RESULTS OF ANALYSIS

A. TOTAL AREAL COVERAGE

The first technique employed to attempt identification of mesoscale precipitation areas involved the use of the total areal coverage on a given map as a function of intensity. The total area was plotted on a log scale with the dbZ scale linear since it is already logarithmic with respect to reflectivity. For practically all maps considered, the curves were very similar. Examples for three maps are shown in Figure 3. As can be seen from the plots, although the range of intensity, areal coverage, and storm type varied, the curves all showed a regular increase in areal coverage as the intensity decreased from the peak value to the base contour with no obvious breaks or kinks. The curves were fairly flat at the higher intensities with increasing curvature as the intensity decreased.

The fact that there were not kinks in the curves was significant in itself. The implication was that there are <u>not</u> certain intensities at which the area changes drastically as opposed to other intensities. If the precipitation structure were such that the mesoscale areas as recognized from photographic data were plateaus of intensity with relatively steep gradients at the edges, one would anticipate large changes in areal coverage at the plateau intensities and fairly constant areal covereage at the intensities where the gradient was steep. These special intensity levels could then be used to identify the threshold for different types of mesoscale phenomena. However, no such kinks were observed and it was apparent that this technique could

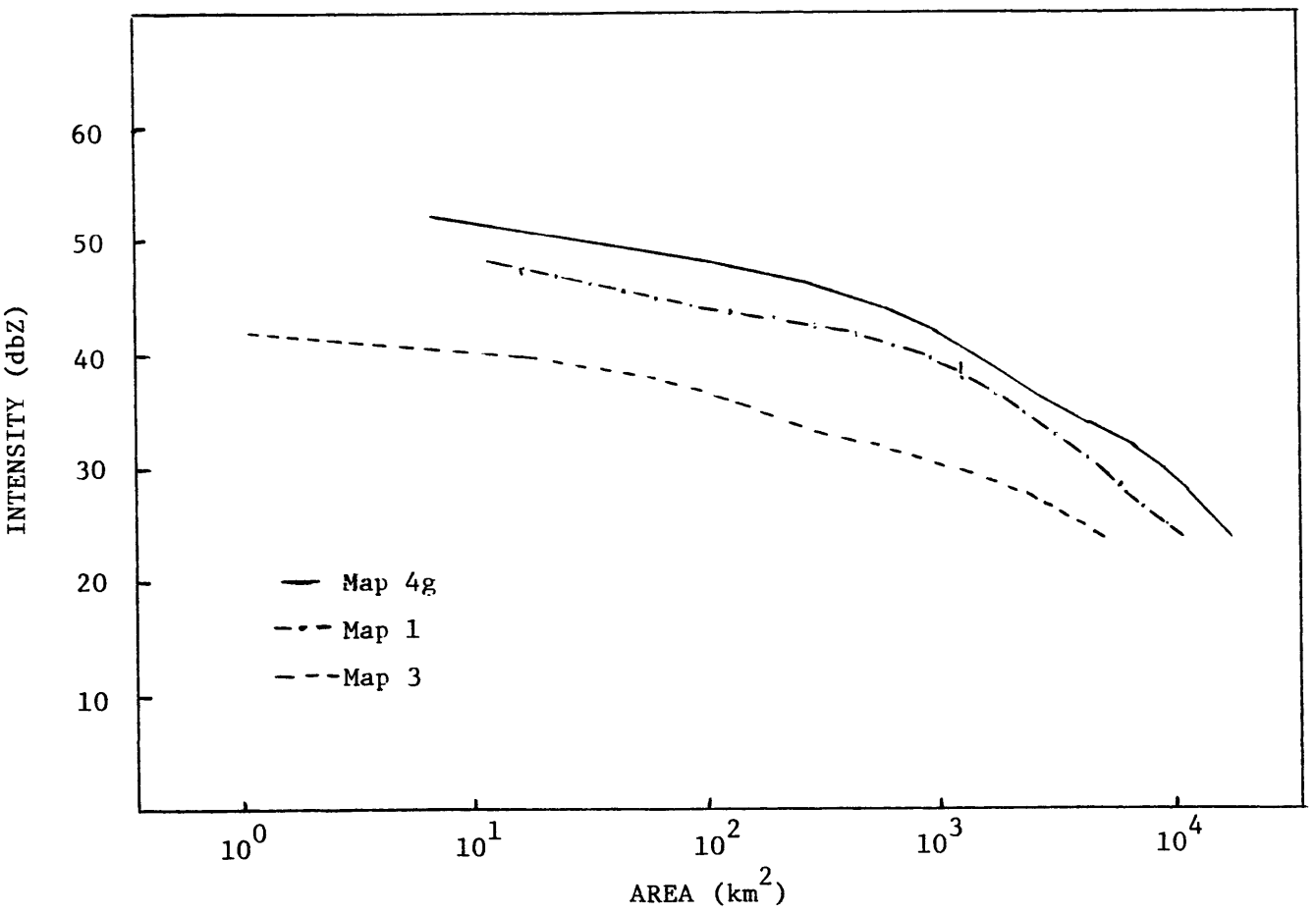

Figure 3. Examples of total areal coverage as a function of intensity for three maps

not be used to identify mesoscale precipitation areas.

B. NUMBER OF AREAS

The distribution of the number of areas identified as a function of intensity could be used in an ideal sense to indicate transition thresholds between different sizes of mesoscale phenomena. If the distribution showed a decrease in number of areas at some intensity threshold, then the implication would be that several areas were merged at that threshold value. Therefore, one could use such decreases to determine thresholds at which a tendency existed for several smaller areas to be merged into a single larger one.

The number of areas observed at each intensity threshold was plotted for each map processed. This total number of areas was subdivided manually into three categories: (1) the number of new areas identified at that threshold (those which did not contain any precipitation of higher intensity); (2) the number of areas which had been identified at a higher threshold and maintained their identity; and (3) the number of areas which were the result of the merger of two or more areas which had been identified at a higher threshold. For each of the areas in the third group, the number of areas identified at the next higher threshold which were merged to form it was determined.

There is one systematic effect which can serve to cause more areas to be found at a given intensity threshold than physically exist. Each dbZ value on a digital map is a result of an averaging process

by the radar and associated instrumentation. The raw signal returned to the radar by precipitation is very noisy. There are frequency fluctuations in the signal caused by interference in the waves scattered from the moving hydrometeors. The standard deviation in this signal is on the order of 6 db. Averaging 32 pulses in time and considering each pulse as an independent sample reduces the standard deviation to slightly over 1 db. As a result of these fluctuations, some of the dbZ values on a map will indicate that the precipitation is of a higher intensity than it actually is and some will indicate lower intensities than actually exist. Consequently, in any rather large area of precipitation of fairly uniform intensity (i.e. low intensity gradient), some of the dbZ values will be higher and some lower than the actual uniform intensity warrants. Therefore, at a threshold intensity just slightly higher than the actual uniform intensity of the large area, small areas would appear randomly because of the signal fluctuations. The result is that more areas could be found than physically exist since the many small areas would really be parts of the single larger area of uniform intensity. This signal break-through phenomenon can be found wherever intensity gradients are weak such as on the trailing edge of a squall line or in the widespread uniform precipitation characteristic of cyclonic storms.

The number of areas observed as a function of intensity is shown in Table 3 for the 24 maps considered. The plot obtained from this data for map 4k is shown in Figure 4. The general shape of the plots

Table 3. Total number of areas observed at each intensity threshold for each map

	MAP																						
DBZ	1	2	3	4a	4b	4c	4d	4e	4f	4g	4h	4i	4j	4k	41	4m	4n	4o	5a	5b	5c	5d	5e	5f
54												1												
52				1		1	2		1	1		1	2	1										
50				2		1	5	1	2	4	1	2	2	2	2	1	1	1						
48	1	1		5	3	2	5	7	9	9	5	8	7	7	5	2	5	2						
46	4	3		7	6	9	10	11	12	17	18	21	12	18	10	4	9	7						
44	6	8		10	8	12	14	14	16	25	28	26	26	19	18	12	8	10				1	1	
42	12	11	1	12	12	15	21	25	18	25	31	30	31	24	19	15	12	11			1	2	3	1
40	16	12	3	13	18	21	30	28	27	30	35	29	31	26	23	19	16	15			2	3	5	3
38	18	12	1	9	15	24	30	33	35	29	42	22	29	25	25	31	28	29	1	8	6	4	8	7
36	20	20	11	10	14	26	32	31	37	43	42	31	20	26	21	31	26	26	8	12	11	12	11	12
34	20	30	23	12	15	25	37	34	37	38	41	22	30	32	35	44	39	41	15	16	18	19	19	15
32	22	33	41	14	17	28	36	40	43	36	40	21	28	36	40	43	51	45	31	29	23	19	17	28
30	21	37	54	17	22	32	35	39	42	33	30	16	27	40	45	30	34	37	23	25	25	18	25	39
28	20	55	54	20	21	34	35	32	38	28	26	16	16	27	37	27	32	36	31	30	20	27	32	27
26	17	53	56	22	28	33	31	35	31	29	21	10	13	25	33	27	28	37	34	34	24	29	26	35
24	11	12	50	28	40	30	31	33	29	36	23	17	16	15	37	41	35	59	41	37	41	29	20	29

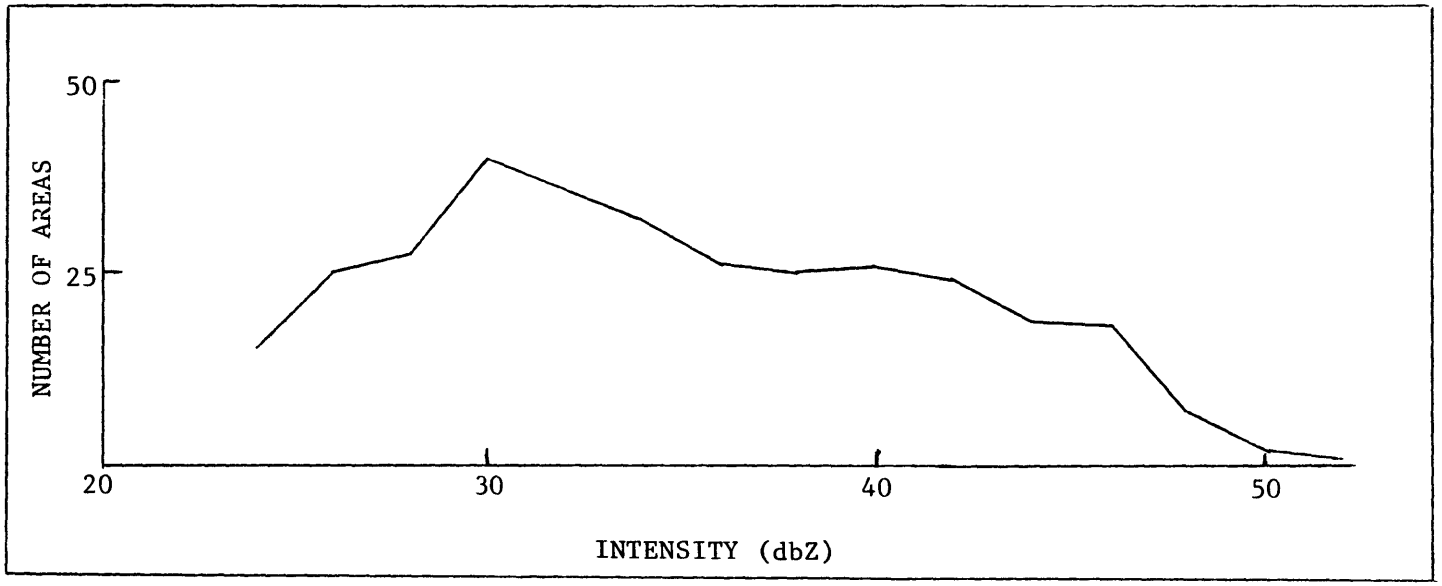

Figure 4. Distribution of the number of areas with intensity for map 4k

obtained for all maps was the same. As the intensity decreased from the peak value on a given map, the number of areas identified increased rapidly at first and then more gradually to a peak value before starting to decrease. At all but the higher intensities, a large number of areas were found.

The September '74 storm (#1) showed a rather steady increase in the number of areas from 1 at 48 dbZ to a peak of 22 at 32 dbZ followed by a steady decline. The peak near 32 dbZ was rather broad and flat. However, in the December case (#2) the peak was rather marked and located at 26-28 dbZ (53 and 55 separate areas, respectively) with a sharp decline at 24 dbZ (12 areas). In the April storm (#3), the number of areas increased from 1 at 42 dbZ to 3 at 40 dbZ and then declined to 1 again at 38 dbZ. Thereafter, the plot increased steadily to a broad peak which began at 30 dbZ and was centered at 28 dbZ. A slight decrease in the number of areas was observed at 24 dbZ. In these three storms, a peak was observed in the vicinity of 30 dbZ with a decrease in the number of areas at lower intensities.

A similar distribution of the number of areas observed at each intensity threshold was obtained for the July squall line. The plots for this storm (#4a-4o) showed a rapid rate of increase in the number of areas from the peak intensity down to near 40 dbZ with a minor peak in the distribution between 38 and 42 dbZ on 10 of the 15 maps. The number of areas then continued to increase at a slower rate to a major peak near 30 dbZ with a peak between 28 and 32 dbZ being observed on 10 of 15 maps. Once again, on nearly all the maps

for this storm, a peak in the number of areas was observed near 30 dbZ. The September '75 storm (#5a-5f) showed similar behavior with a peak observed between 28 and 32 dbZ on all 6 maps.

In general the distribution of the number of areas with respect to intensity was very similar for all maps and the preferred threshold intensities for a peak in the number of areas were in the vicinity of 30 dbZ. In order to gain further insight into the distribution of the number of areas with intensity, the total number of areas at each intensity threshold was subdivided into the three categories mentioned above (i.e., new, same, and result of merger). The results of this subdivision are given in Tables 4, 5, and 6. The information from these three tables has been consolidated for selected maps in Table 7 for easier reference.

At the higher intensities most of the areas at each threshold were new areas for all storms. In the cyclonic storms (#2,3,5e), the number of new areas continued to dominate at all intensities. However, in the two squall line storms(#1,4f), there was some critical intensity threshold below which the number of new areas was smaller than the number which retained their identity. This can be explained by considering the degree of organization of the two types of storms. Squall lines are highly organized storms with the precipitation by definition confined to a rather limited area either side of the line itself. Squall lines are also characterized by rather strong intensity gradients especially along the leading edge. On the other hand, cyclonic storms are characterized by rather widespread precipitation

Table 4. Number of new areas identified at each intensity threshold for each map

	MAP																						
DBZ	1	2	3	4a	4b	4c	4d	4e	4f	4g	4h	4i	4j	4k	4l	4m	4n	4o	5a	5b	5c	5d	5e	5f
54												1												
52				1		1	2		1	1		0	2	1										
50				1		0	3	1	1	3	1	1	1	1	2	1	1	1						
48	1	1		3	3	1	1	6	7	6	4	7	5	5	3	1	4	1						
46	3	2		2	3	7	5	5	4	8	13	15	6	11	6	2	4	5						
44	2	6		3	3	4	4	3	5	12	13	9	17	4	10	9	1	5				1	1	
42	6	7	1	3	4	4	9	11	5	8	10	7	11	9	4	7	6	3			1	1	2	1
40	5	7	2	3	7	8	11	7	10	9	12	7	9	7	7	6	6	6			1	1	3	2
38	6	6	0	0	1	4	6	8	15	7	12	6	7	4	6	13	17	15	1	8	4	2	6	5
36	3	13	10	3	1	4	4	3	12	20	14	13	9	8	5	9	9	8	7	6	7	11	6	8
34	5	16	16	2	2	3	8	7	18	14	14	7	10	14	17	26	20	19	10	9	9	12	12	9
32	8	15	24	2	3	9	7	14	16	14	16	9	9	16	15	16	27	14	19	18	15	9	7	20
30	5	19	33	5	6	7	9	12	8	9	6	5	17	20	22	9	7	9	10	9	12	8	16	18
28	7	33	26	5	3	7	9	7	8	8	6	7	9	11	12	9	14	8	13	13	7	15	16	5
26	6	42	25	3	8	8	9	8	10	7	6	3	7	12	16	12	9	10	13	17	11	13	15	19
24	4	10	23	12	21	11	12	11	13	15	15	9	8	6	21	11	16	33	24	19	23	18	8	13

Table 5. Number of areas at each intensity threshold which maintained their identity from the next higher intensity threshold

	MAP																						
DBZ	1	2	3	4a	4b	4c	4d	4e	4f	4g	4h	4i	4j	4k	4l	4m	4n	4o	5a	5b	5c	5d	5e	5f
54																								
52												1												
50				1		1	2		1	1		1		1										
48				2		1	2	1	2	2	1	0	2	2	2	1	1	1						
46	1	1		5	3	2	5	5	7	9	5	4	5	7	3	2	5	2						
44	4	1		7	4	7	10	11	10	10	12	13	8	12	7	2	6	4						
42	6	2		8	8	10	10	14	11	12	14	20	14	12	14	6	4	6				1	1	
40	10	3	1	8	10	11	17	18	16	18	18	16	15	16	14	11	8	7			1	2	1	1
38	9	2	0	8	11	19	19	22	14	18	27	9	15	16	16	17	8	13			2	1	0	1
36	16	5	1	5	12	20	26	24	22	18	19	15	13	13	13	13	12	16	1	4	3	0	3	2
34	12	11	6	10	12	18	27	24	27	15	20	7	14	13	15	13	14	19	3	4	7	5	6	3
32	9	12	15	12	13	14	24	21	22	17	18	8	13	15	16	18	16	24	10	8	2	5	5	6
30	12	13	11	10	15	22	23	20	30	22	21	7	7	14	15	14	17	22	8	13	9	6	5	17
28	9	18	21	13	14	24	22	18	23	14	16	6	5	8	20	16	14	22	14	11	7	8	10	15
26	8	6	21	18	19	22	17	23	15	19	11	4	3	10	14	13	13	21	14	10	9	10	6	11
24	3	1	19	13	16	14	14	19	13	16	6	6	7	7	12	3	17	23	13	14	16	5	6	10

Table 6. Number of areas identified at each intensity threshold which were formed by merger of two or more areas which had been identified at the next higher intensity threshold

	MAP																							
DBZ	1	2	3	4a	4b	4c	4d	4e	4f	4g	4h	4i	4j	4k	4l	4m	4n	4o	5a	5b	5c	5d	5e	5f
54													1											
52																								
50							1			1		1	0											
48							0	1	1	0		2	1		1									
46		1			1	1	0	0	1	3	3	4	2	2	1	1	1	1						
44		2		1	0	1	2	0	2	5	7	3	6	3	1	2	2	2						
42	1	2		2	1	2	2	3	1	3	5	6	7	3	2	2	2	2					1	
40	3	4	1	1	3	1	5	3	6	4	3	7	7	5	3	1	3	1				1	2	1
38	1	2	0	2	1	2	2	4	3	5	9	3	8	5	3	9	5	2		2	1	1	2	2
36	3	3	1	0	1	4	2	3	2	9	7	8	6	5	3	5	5	3	2	3	2	2	1	3
34	5	6	2	0	1	5	5	5	5	5	6	4	6	5	9	9	8	7	2	3	6	5	5	2
32	4	5	10	2	1	3	3	7	4	2	3	4	3	6	8	7	10	6	5	3	4	4	4	4
30	4	4	7	2	4	3	4	6	7	6	4	3	2	8	5	2	4	6	4	6	6	4	6	7
28	3	5	10	1	1	3	5	4	6	3	4	3	3	3	3	2	6	6	7	7	4	6	5	5
26	4	1	8	3	3	5	5	3	3	5	2	2	1	2	4	3	2	3	4	4	2	6	6	6
24																								

Table 7. Consolidation of Tables 4, 5, and 6 for five maps. The columns labled N, S, and M represent the number of new areas, areas which retained their identity, and areas which resulted from merger at each intensity threshold, respectively.

MAP	1 SQUALL LINE			2 CYCLONIC STORM			3 CYCLONIC STORM			4f SQUALL LINE			5e CYCLONIC STORM		
DBZ	N	S	M	N	S	M	N	S	M	N	S	M	N	S	M
52										1					
50										1	1				
48	1			1						7	2				
46	3	1		2	1					4	7	1			
44	2	4		6	1	1				5	10	1	1		
42	6	6		7	2	2	1			5	11	2	2	1	
40	5	10	1	7	3	2	2	1		10	16	1	3	1	1
38	6	9	3	6	2	4	0	0	1	15	14	6	6	0	2
36	3	16	1	13	5	2	10	1	0	12	22	3	6	3	2
34	5	12	3	16	11	3	16	6	1	18	27	2	12	6	1
32	8	9	5	15	12	6	24	15	2	16	22	5	7	5	5
30	5	12	4	19	13	5	33	11	10	8	30	4	16	5	4
28	7	9	4	33	18	4	26	21	7	8	23	7	16	10	6
26	6	8	3	42	6	5	25	21	10	10	15	6	15	6	5
24	4	3	4	10	1	1	23	19	8	13	13	3	8	6	6

of weak intensity gradient. Therefore, as the intensity threshold decreases from the peak value on a given map, new areas would be more likely to be found in cyclonic storms for two reasons. The first is the fact that the area covered by precipitation at a lower threshold in a squall line would most likely be in the form of growth onto an already existing area because of the compactness of the storm. However, in a widespread cyclonic storm, the area covered by precipitation at a lower threshold would have a far greater likelihood of being quite distant from existing areas. The second reason is that the signal break-through phenomenon would be more prevalent in a cyclonic storm than in a squall line because the intensity gradients are generally much weaker. Therefore, one would be more likely to find areas which were a result of signal fluctuations rather than meteorological variations in a cyclonic storm. Although new areas were found at virtually all intensity thresholds on all the maps, the fact that the distribution of the total number of areas showed peaks indicated that merging was a significant process in both types of storms.

According to Tables 6 and 7, significant merging began to occur about 8-10 dbZ below the peak intensity on nearly all maps. In order to determine how many of the areas at one intensity threshold were influenced by merger at the next lower threshold, the reduction in number of areas as a result of merger from one threshold value to the next lower value was determined. For example, if an area identified at 34 dbZ was a result of merger of three areas which had been identified at 36 dbZ, then a total reduction of two occurred in the

number of areas from 36 to 34 dbZ as a result of merger. Table 8 shows the variation with intensity of reduction in number caused by mergers for all 24 maps. The general trend was for the reduction by merger to increase with decreasing intensity with few exceptions. Eventually, a threshold was reached at which the reduction by merger exceeded the number of new areas found. This resulted in the peak in the total number of areas which was observed on practically all maps.

The threshold region at which this peak in the number of areas was observed could be considered significant for defining mesoscale areas. The fact that the total number of areas continued to decrease for intensity thresholds below the point at which the peak was observed (i.e. in the vicinity of 30 dbZ) indicated that the merging process continued to dominate the appearance of new areas. Most of the precipitation at the lower intensities then was in the form of growth on existing areas rather than in the form of new areas. Therefore, it would be reasonable to assume that the important large precipitations areas in a storm could be defined by the threshold at which the merging process began to dominate the number of new areas. The growth occurring below this threshold would then serve to incorporate insignificant existing areas as well as insignificant new areas found at these lower thresholds into the more important areas. The problem with such a method of defining mesoscale areas is that the thresholds in the vicinity of 30 dbZ outlined a large number of areas with a wide range of characteristics. This pointed to the need for a significance criterion which would be able to distinguish the important areas and

'able 8. Reduction in number of areas at each intensity threshold as a result of merger

	MAP																					
.	2	3	4a	4b	4c	4d	4e	4f	4g	4h	4i	4j	4k	41	4m	4n	4o	5a	5b	5c	5d	5e
												1										
						1			1		1	0										
						0	1	1	0		2	1		1								
	1			1	1	0	0	1	4	3	4	2	2	2	1	3	2					
	4		1	0	1	2	0	3	8	7	3	7	4	3	4	2	2					
L	6		2	1	2	2	4	1	4	8	8	9	5	3	2	2	2					1
ł	6	2	4	4	1	6	3	7	8	5	13	8	5	4	1	5	1				1	3
L	5	0	2	2	2	2	5	10	6	14	4	8	6	9	9	11	9		2	2	3	3
5	6	4	0	1	4	3	3	8	21	15	16	10	8	3	13	7	4	3	5	2	5	4
5	12	6	0	1	6	8	8	10	16	17	10	8	12	10	17	15	10	3	5	10	9	9
5	19	20	2	1	3	9	13	9	12	16	10	17	16	15	22	29	17	18	13	10	9	8
3	15	26	2	4	5	8	14	12	13	10	7	20	24	20	12	16	9	5	8	12	6	9
9	44	23	1	1	9	13	5	17	6	11	9	10	12	20	12	13	9	10	13	7	11	21
10	51	29	6	9	14	12	13	19	8	13	2	5	16	17	14	9	11	17	16	6	18	14

eliminate the unimportant ones. More will be said about this problem of significance later.

The overall distribution of the number of areas with intensity threshold can be described than in terms of the appearance of new areas and merging. As the intensity threshold is decreased from the peak intensity, the total number of areas increases rapidly because new areas are appearing and merging has not yet become important. Some 8-10 dbZ below the peak intensity, significant merging begins to occur and the increase in the total number of areas slows. At some critical intensity threshold, the merging phenomenon becomes dominant and produces a peak in the total number of areas distribution. The most common peak for all the storms considered occurred in the vicinity of 30 dbZ with a minor secondary peak at the 38-40 dbZ threshold in the intense July '75 squall line.

C. AREA SIZES

At each intensity threshold, the areas identified were histogrammed according to size with the class intervals chosen geometrically to number 8 as follows:

Class	Size Interval	
	(nm^2)	(km^2)
I	$0 < x < .5$	$0 < x < 1.7$
II	$.5 \leq x < 2$	$1.7 \leq x < 6.9$
III	$2 \leq x < 8$	$6.9 \leq x < 28$
IV	$8 \leq x < 32$	$28 \leq x < 110$
V	$32 \leq x < 128$	$110 \leq x < 440$
VI	$128 \leq x < 512$	$440 \leq x < 1760$
VII	$512 \leq x < 2048$	$1760 \leq x < 7030$
VIII	$2048 \leq x < 8192$	$7030 \leq x < 28100$

It was hoped that the preferred size interval would remain about the same over a wide range of intensity thresholds with jumps to larger size intervals at threshold values which could then be used to identify mesoscale areas. However, the preferred areal sizes in all cases were the smaller class intervals and rarely exceeded Class III. Table 9 shows the results for two maps.

At all but the higher intensity thresholds there was a wide range of areal sizes with no clear breaks in the data. At the higher intensities, all the areas were small. At the medium and lower intensity thresholds, there were a few large areas with many small areas which resulted in the preferred areal sizes being small. Also, the mean areal size was usually considerably smaller than the maximum areal size at a particular threshold. This strong similarity at all thresholds suggested that a consideration of sizes alone could not indicate thresholds which could be used to define mesoscale areas.

An attempt was then made to use the area sizes in such a way as to locate thresholds which were important in the merging process. One parameter which was examined was ln (maximum areal size/mean areal size). This parameter was evaluated at each intensity threshold and was found to increase with decreasing intensity as indicated by the sample distribution shown in Figure 5. Such behavior can be explained by considering the merging process. Mergers would serve to increase both the maximum areal size and the mean areal size. However, the greater effect would be on the maximum size since the mean areal size would be more strongly affected by the large number of small areas

Table 9. Number of areas in each size class interval for each threshold value for maps 2 and 4o. Underscored numbers represent preferred class interval.

MAP 2

DBZ	I	II	III	IV	V	VI	VII	VIII
50								
48	0	1						
46	2	0	1					
44	2	1	4	1				
42	1	0	8	1	1			
40	4	2	3	1	1	1		
38	5	2	0	2	2	1		
36	11	3	1	1	2	2		
34	9	10	5	1	3	2		
32	14	11	1	2	3	2		
30	18	8	7	0	0	4		
28	36	7	8	1	0	2	1	
26	30	16	3	1	0	2	1	
24	10	1	0	0	0	0	0	1

MAP 4o

DBZ	I	II	III	IV	V	VI	VII	VIII
50	0	1						
48	0	1	1					
46	0	3	4					
44	0	5	4	1				
42	0	3	5	3				
40	0	4	6	4	1			
38	0	10	8	9	2			
36	0	11	5	8	1	1		
34	0	22	9	5	3	1	1	
32	1	13	17	4	8	1	1	
30	1	9	15	6	3	2	1	
28	1	9	14	3	6	1	2	
26	1	8	16	5	3	1	3	
24	1	25	22	6	2	1	2	

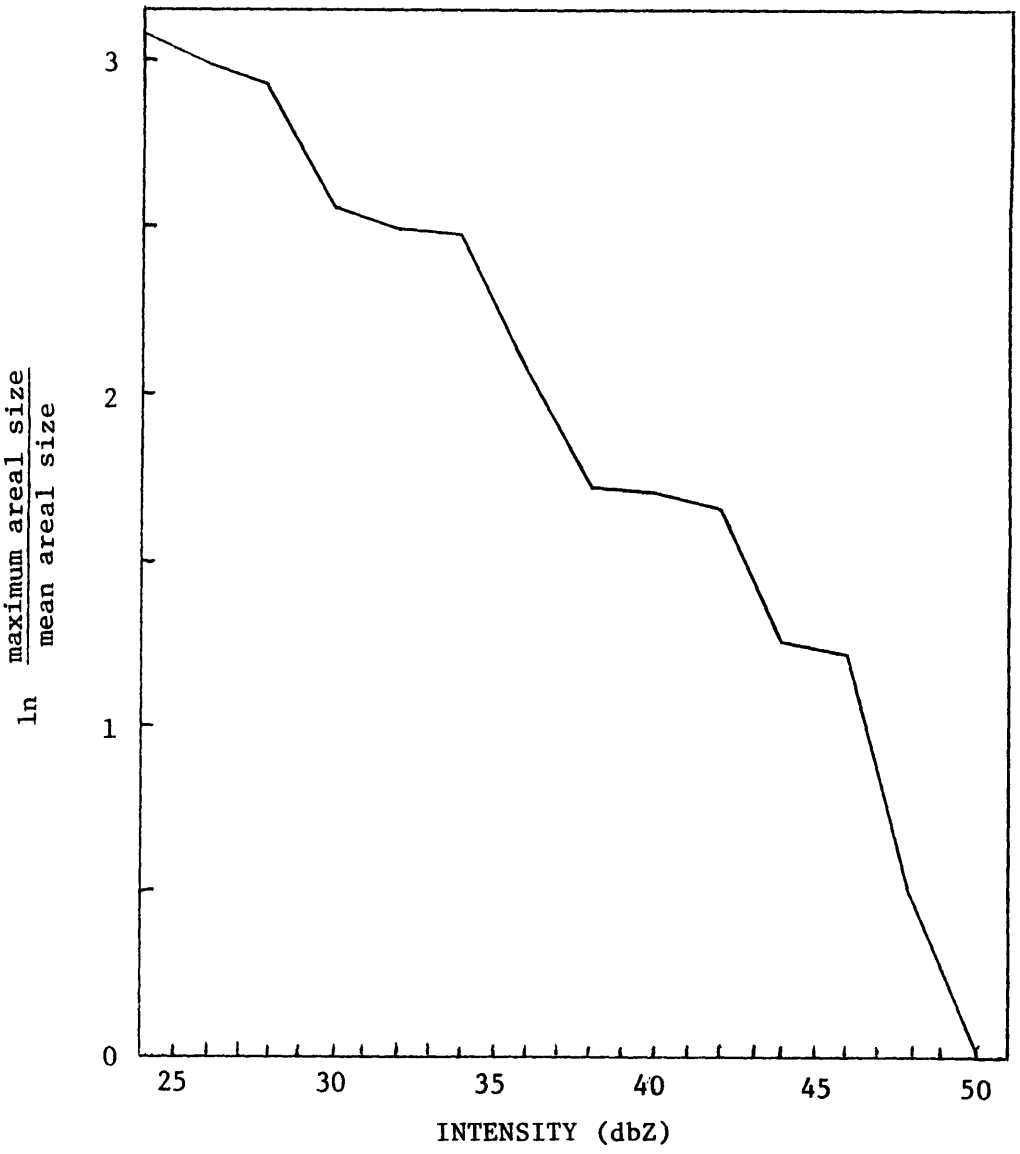

Figure 5. Distribution of ln ($\frac{\text{maximum areal size}}{\text{mean areal size}}$) with intensity for map 41

than by changes in the size of the few large areas. Therefore, a sharp increase in the parameter would indicate significant merging. However, this parameter increased more or less steadily without showing recognizable intensities where the merging was especially important.

Since it had been observed that the merging process tended to decrease the number of areas, a parameter F_N given by

$$F_N = \left(\frac{1}{\text{number of areas}} \right) \ln \left(\frac{\text{maximum areal size}}{\text{mean areal size}} \right)$$

could be expected to peak at thresholds where merging was important. Such thresholds could possibly be used to define transistions between LMSA's and SMSA's. This parameter was then examined for each map in an attempt to use the sizes of areas as a criterion to determine which intensity thresholds were important in the merging process.

The quantity F_N did display a distribution which had peaks as shown by the example given in Figure 6. F_N had between two and four peaks for all maps with the peaks identified for each map given in Table 10. Peaks were consistently observed near both ends of the intensity spectrum for each map. These extreme peaks can be explained in terms of the number of areas and mergers. Usually there was only one area identified at the highest intensity for a given map which resulted in the raito of the maximum size to the mean size being one and F_N having the value zero. As the intensity threshold decreased, the maximum areal size was larger than the mean areal size and therefore the quantity F_N took on a value other than zero. However, the number of areas was small enough at the higher intensities to

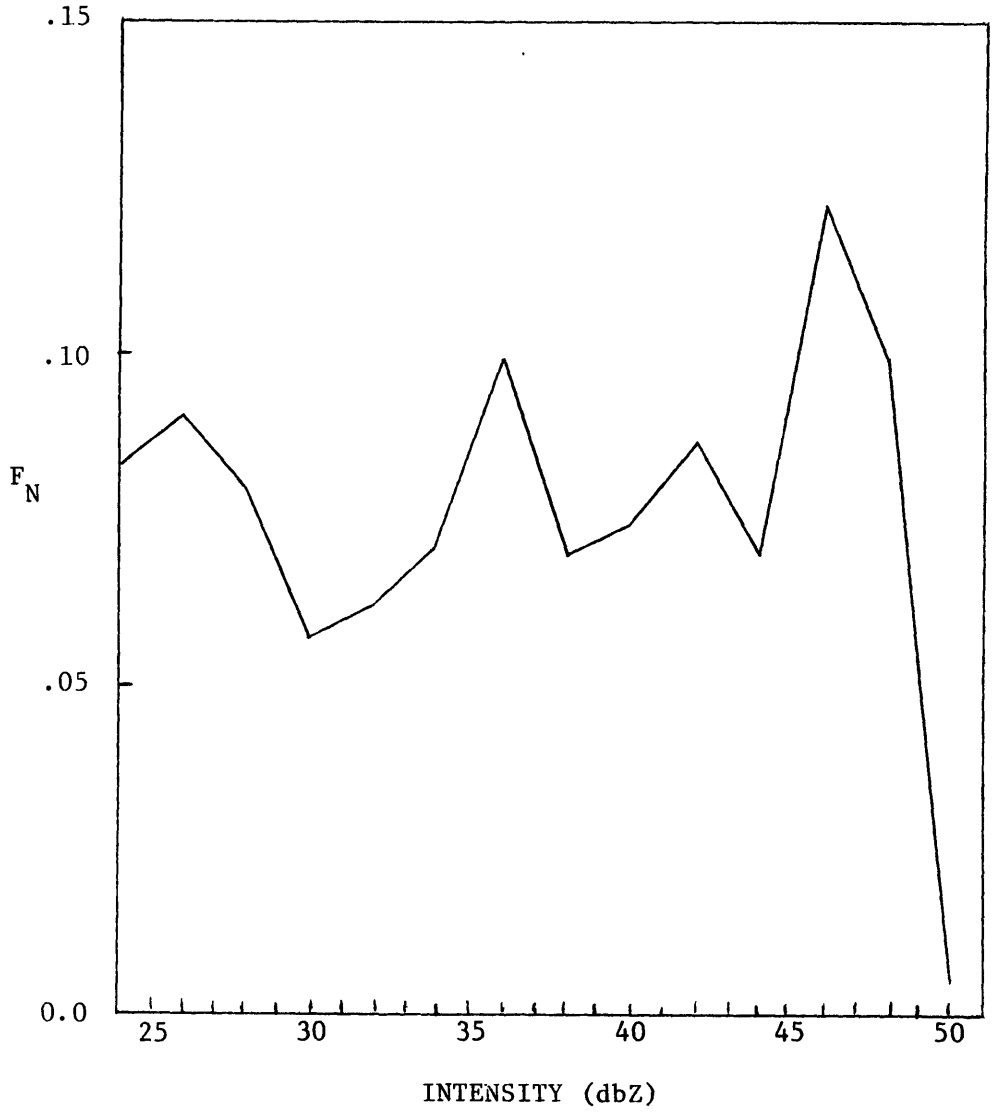

Figure 6. Distribution of F_N with intensity for map 41

Table 10. Intensity thresholds (dbZ) at which F_N showed peaks

MAP	PEAKS AT INTENSITY EXTREMES	MEDIUM RANGE INTENSITY PEAKS
1	24,46	--
2	24,46	38-42
3	24,40	36
4a	--,46	38
4b	28,46	36
4c	24,48	32
4d	24,48	--
4e	24,46	--
4f	24,48	42
4g	28,50	38,42
4h	24,48	--
4i	26,48	38
4j	24,50	38,42
4k	24,50	36
4l	26,46	36,42
4m	26,48	--
4n	26,46	38
4o	28,44	36
5a	24,36	30
5b	24,38	--
5c	28,38	32
5d	24,42	--
5e	24,40	34
5f	24,40	34

cause a peak in F_N. At the lower intensity extreme, the merging process produced a large ratio of maximum to mean areal size as well as a decrease in the number of areas thus producing a peak in F_N.

The medium range intensities at which F_N showed peaks varied from 32 dbZ to 42 dbZ with the tendency being for the more intense storms (#2 and 4) to show peaks at the higher thresholds and the less intense storms (#3 and 5) to have peaks at lower intensities. These medium range peaks defined thresholds at which merging was important and would presumably indicate intensities which could be used to define mesoscale areas. However, the large number of areas and wide range of areal sizes observed at these medium range peak thresholds served to discount the use of the peaks to define mesoscale areas. Also, in the storms where time sequences were available, the medium range peaks identified in F_N were not consistent in time and did not show any pattern of progression. For these reasons, the F_N analysis did not indicate <u>exact</u> thresholds which could be used to define mesoscale areas. Nonetheless, the analysis did indicate that thresholds in the middle to upper thirties seemed to be more important than others in the merging process. The 36-38 dbZ range was chosen as being the most suitable for both the more and less intense storms.

The size distribution analysis discussed in this section indicated that at all but the higher intensity thresholds there existed a wide range of areal sizes with a preference for the smaller sizes in all cases. At the higher intensities, all the areas were small. At the medium and lower intensities, there were a few large areas and many

small areas which resulted in the preference for smaller sizes and also caused the mean areal size to be much smaller than the size of the few large areas. Although the analysis of the parameter F_N did not indicate exact thresholds which could be used to identify mesoscale phenomena, it did indicate that intensity thresholds in the 36-38 dbZ range seemed to be more important than other medium range thresholds for merging. The number of areas analysis which was discussed in the previous section indicated significant merging occurred in the vicinity of 30 dbZ.

Both the preference for small sizes and the wide range of sizes observed at the 30 dbZ and 36-38 dbZ intensity ranges indicated that there was a need for some measure of significance to differentiate between important and unimportant areas. In past analyses of mesoscale precipitation areas, selection for study had been on the basis of retention of identity over a period of time. However, for a single map the significance of a given area would be expected to depend on its size and its intensity. Since no clear breaks could be observed in the data which would serve as a natural significance criterion, it was decided to pick the 5 largest areas at a given intensity threshold as being the most significant. This choice was completely arbitrary but, as will be shown in a later section on significance of areas, not unreasonable. This significance criterion indicated that the average size of a significant area at the higher selected intensity threshold which would presumably define SMSA's was $155km^2$. This is an acceptable size for small mesoscale areas according to the

definitions of Austin and Houze (1972). The average for the lower selected threshold was 879km^2 which is slightly less than their defining value of 1000km^2 for LMSA's but is not unreasonable. It should be noted, however, that these values were averages of sets of numbers which showed considerable variation and although the sizes are acceptable, they by no means verify that the entities defined by these thresholds are the same entities called large and small mesoscale areas by previous investigators. Only analysis of time sequences in many more storms will finally reveal whether or not these entities are the same as the previously observed LMSA's and SMSA's. The fact that the sizes are within the appropriate range indicates that thresholds in the vicinity of 30 dbZ and 36-38 dbZ are reasonable ones to choose in further studies of mesoscale areas.

D. THE DISTRIBUTION OF AREA WITH INTENSITY

The similarity and behavior of the plots of total areal coverage on a map as a function of intensity led to the hypothesis that perhaps a simple relation could be found which would describe the area covered as a function of the intensity. Some preliminary experiments by Austin and Morrow (1975) indicated the fourth root of the total areal coverage by precipitation in excess of a given intensity threshold could be linearly related to intensity. Several relations were tested on the storms in this study including square root, cube root, fourth root and log of area. The relations are shown in Figure 7 for map 1. The fourth root described the most linear relation for this

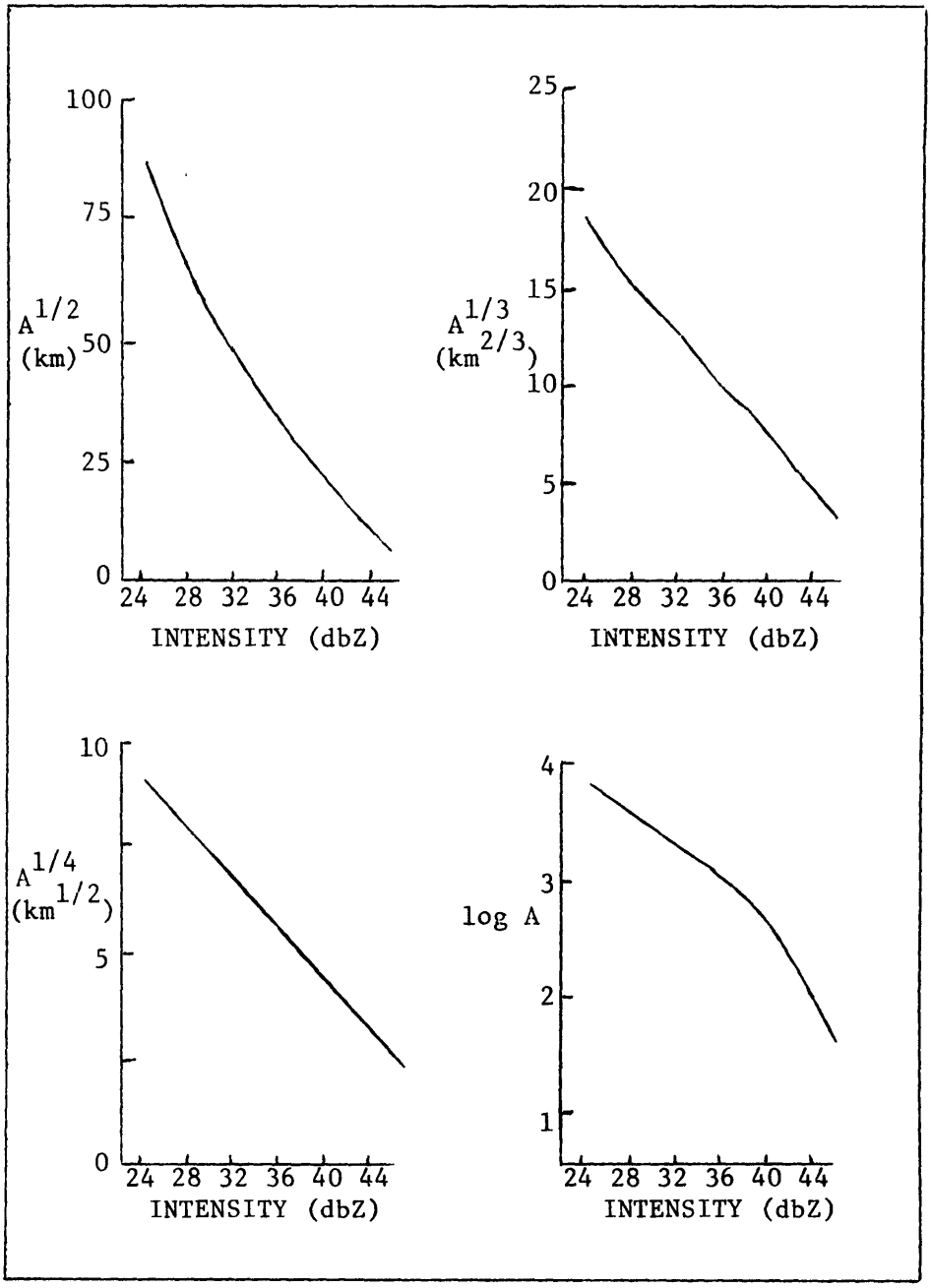

Figure 7. Example of area scales tried to describe the distribution of area with intensity for map 1

map as well as for other maps as can be seen in Figure 8. Because the total area covered by precipitation in excess of a given intensity threshold could be related to the intensity on a map as a whole, it was decided to see if the relation held for individual precipitation areas.

In order to make this determination, each individual area at each intensity threshold on a map was matched manually to the area with which it was associated at the next lower threshold value. This was accomplished by numbering the areas starting with the highest intensity value found on the map and then matching each area at the higher intensity (using the centroids as much as possible) to the corresponding area at the next lower intensity. When two or more areas identified at the higher threshold were merged at the lower threshold, the new area was designated by the identification number of the merging area which contained the highest peak. This stratification was accomplished for all intensities from the peak value on the map down to and including 24 dbZ. An example of such a stratification is shown in Table 11.

It was observed that if the fourth root of the cumulative areal coverage within a given precipitation area was plotted as a function of intensity, the relationship described was a more or less linear one for areas identified in all the storms, as can be seen in Figure 9. Therefore, it was possible to write

$$(A_Y)^{1/4} = MY + B$$

where A_Y was the area covered by precipitation with intensity equal

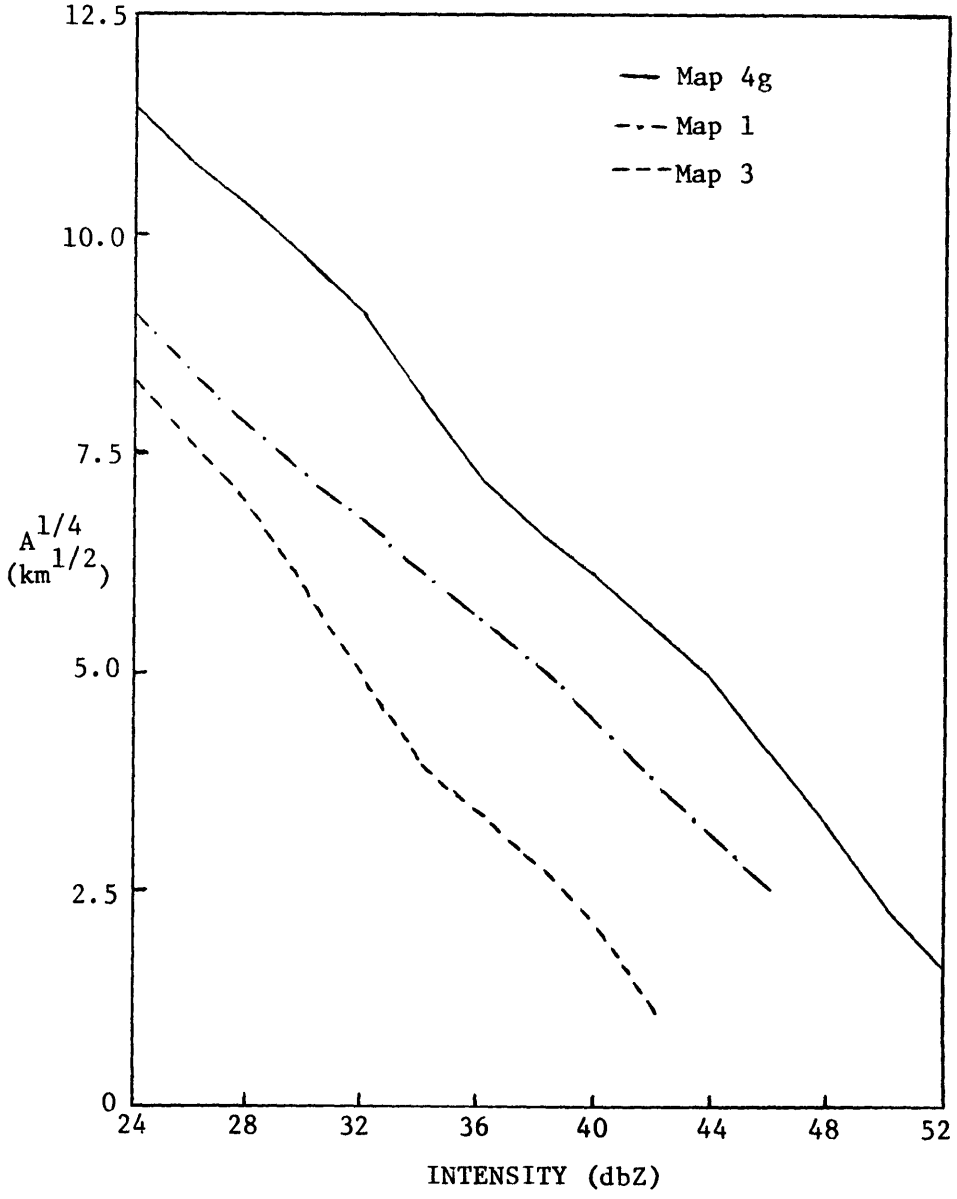

Figure 8. Distribution of the fourth root of areal coverage with intensity for three maps

Table 11. Stratification of areal coverage in km^2 at each intensity threshold for each area identified on map 5a. Underscoring indicates area was merged into area numbered in parenthesis at that intensity threshold. For example, area 18 became part of area 2 at the 24 dbZ threshold.

AREA NUMBER

DBZ	1	2	3	4	5	6	7	8	9	10	11	12	13	14	15	16	17	18	19	20
38	3.06																			
36	21.3	7.08	20.3	2.58	52.2	16.6	3.06	6.11												
34	46.0	14.0	88.9	(3)	188.	188.	(6)	(6)	20.2	10.5	54.2	5.94	16.9	54.9	5.39	20.7	5.53	8.28		
32	223.	42.2	(1)		755.	(5)			45.3	31.6	176.	11.9	79.6	93.4	38.1	72.1	(5)	16.4	4.09	17.5
30	384.	118.			1267				872.	90.0	(9)	(9)	(9)	(5)	118.	(15)		69.3	4.09	(1)
28	518.	160.			1549				1453	(9)					253.			89.6	23.9	
26	721.	222.			1882				2370						337.			218.	27.9	
24	1112	6426			(2)				(2)						491.			(2)	60.1	

DBZ	21	22	23	24	25	26	27	28	29	30	31	32	33	34	35	36	37	38	39	40
32	2.88	3.78	50.8	7.08	4.36	37.7	4.43	8.59	4.57	5.56	10.2	5.94	5.46	3.11	19.6	7.55	3.53			
30	(1)	(1)	132.	(2)	(9)	(9)	(9)	(9)	(9)	(9)	37.7	35.0	10.9	57.0	(5)	(5)	(5)	19.8	8.58	7.96
28			248.								79.3	118.	43.9	121.				51.8	25.4	52.5
26			(9)								302.	265.	(32)	(31)				80.0	42.5	76.6
24											(2)	338.						112.	(1)	(2)

DBZ	41	42	43	44	45	46	47	48	49	50	51	52	53	54	55	56	57	58	59	60
30	4.01	3.77	17.9	5.80	7.31	3123	8.82													
28	(40)	18.8	(23)	(23)	40.1	(5)	39.8	8.45	3.06	5.70	11.6	7.41	4.36	2.57	5.77	3.77	13.1	5.53	22.7	4.19
26		41.5			590.		(18)	33.9	(1)	(9)	(9)	17.1	17.5	(5)	(5)	26.6	23.2	22.2	181.	(59)
24		(2)			(2)			73.5				(2)	30.8			(2)	(2)	73.1	391.	

DBZ	61	62	63	64	65	66	67	68	69	70	71	72	73	74	75	76	77	78	79	80
26	4.98	3.60	3.41	13.3	21.0	15.9	2.93	6.66	6.42	6.18	6.35	4.74	50.1							
24	(48)	(2)	(2)	(2)	63.2	(2)	2.93	115.	38.1	18.4	(69)	32.6	128.	12.5	5.80	20.6	6.73	7.48	3.53	6.25

DBZ	81	82	83	84	85	86	87	88	89	90	91	92	93	94	95	96	97
24	15.2	13.8	4.80	4.08	4.19	9.10	6.42	44.6	6.11	6.87	6.25	4.84	6.11	7.00	37.0	30.0	4.91

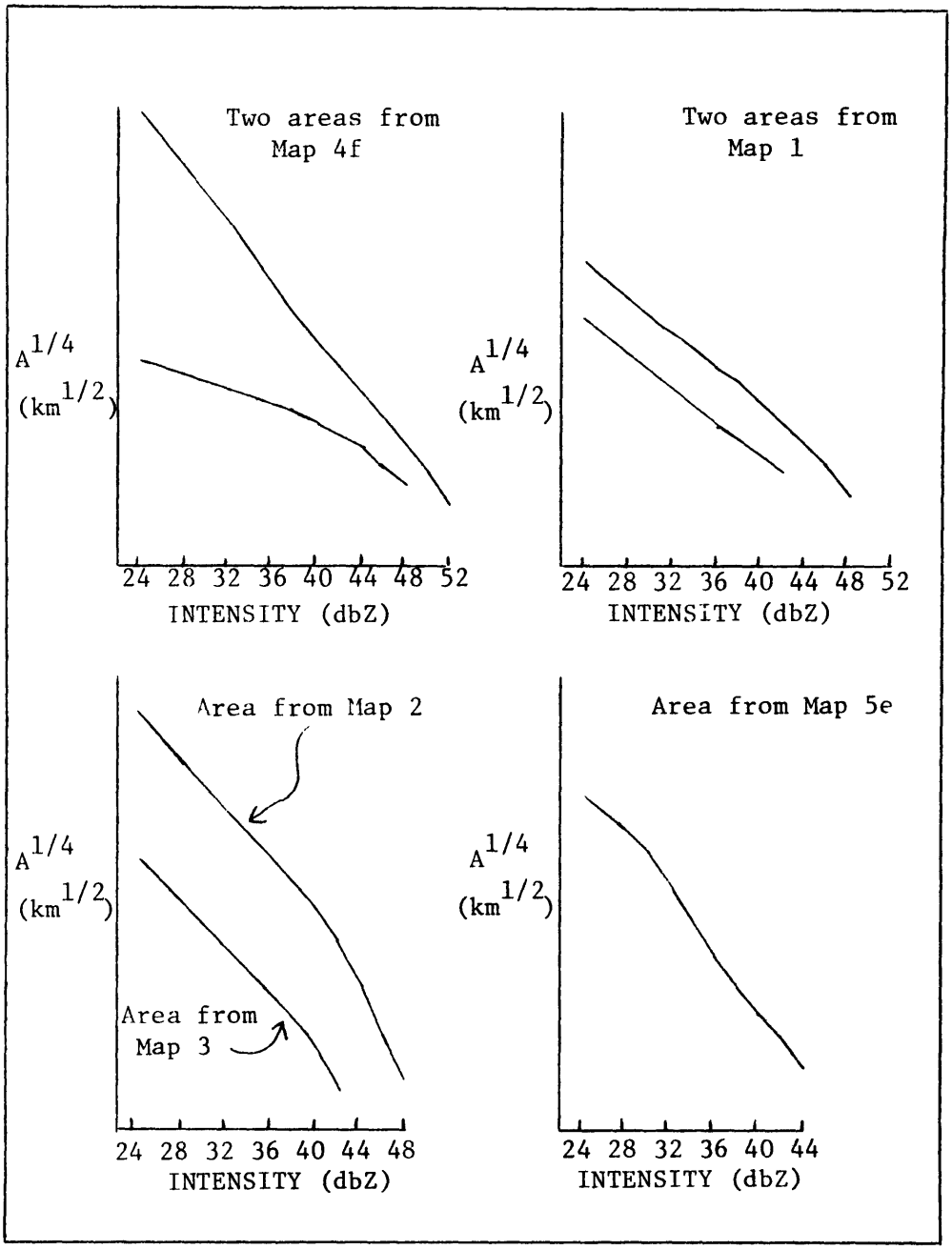

Figure 9. Examples of the distribution of the fourth root of areal coverage with intensity for individual precipitation areas on maps from each storm

to or greater than Y dbZ above the threshold value (i.e., $Y = dbZ - dbZ_{base}$), M the slope and B the intercept. This relationship held for all the storms which were considered and seemed to be the most nearly linear for the larger areas.

Although this concept appeared to be quite useful, it required a knowledge of the behavior of the constants M and B. The precipitation areas identified were of various sizes and intensities and consequently the constants which would best describe the areas would be very different. The constant B could be considered the fourth root of the areal coverage at the threshold intensity. However, because the linear relation was an approximation, the constant as determined from linear regression would show some variability from the actual observed coverage. The slope M would depend on several things: 1) the size of the area under consideration; 2) the magnitude of the peak intensity of the area; and 3) the areal coverage of the peak intensity of the area. For example, consider two areas of the same size. Suppose one area had a peak intensity of 48 dbZ and the other a peak of 52 dbZ. The slopes describing these two areas could be quite different. Similarly, if both had the same peak intensity, but one had a broad flat peak with areal coverage $10km^2$ and the other had a sharply defined peak with an areal coverage of $2km^2$, again the slopes would be different.

In order to determine the dependence of the constants on these factors, an in-depth study of the individual areas in the July '75 (#4) and September '75 (#5) storms was undertaken. For the 15 maps of the

July storm, the largest 4 or 5 areas at 24 dbZ were used. For each of the 69 areas chosen, the constants M and B which best described the actual observed decrease in areal coverage with increasing intensity were determined. Relations were sought which would predict these constants as a function of some easily measurable characteristic of the individual precipitation areas.

The relation between M and the areal coverage at the threshold intensity was investigated first. Each of the 69 values of M was plotted on a scatter diagram against the size of the individual area with which it was associated as shown in Figure 10. The best fit line to predict M in units of $km^{1/2}dbZ^{-1}$ as a function of areal coverage at the threshold intensity was determined to be

$$M = -.019 - .03(A_{base})^{1/4}$$

where the area is expressed in km^2, and this line is shown in the figure. This same technique was used to determine the best prediction formula for B in terms of areal size. The best fit line shown in Figure 11 was found to be

$$B = -.088 + 1.009(A_{base})^{1/4}$$

where the area is again expressed in km^2 and B is in units of $km^{1/2}$. This prediction equation for B in the July '75 storm indicated that the fourth root of the actual size of the area under consideration would be within about 1% of the predicted value for the constant.

In order to see how well these empirical equations worked, several areas were chosen to make comparisons between the observed areal coverage at certain intensity thresholds and the predicted

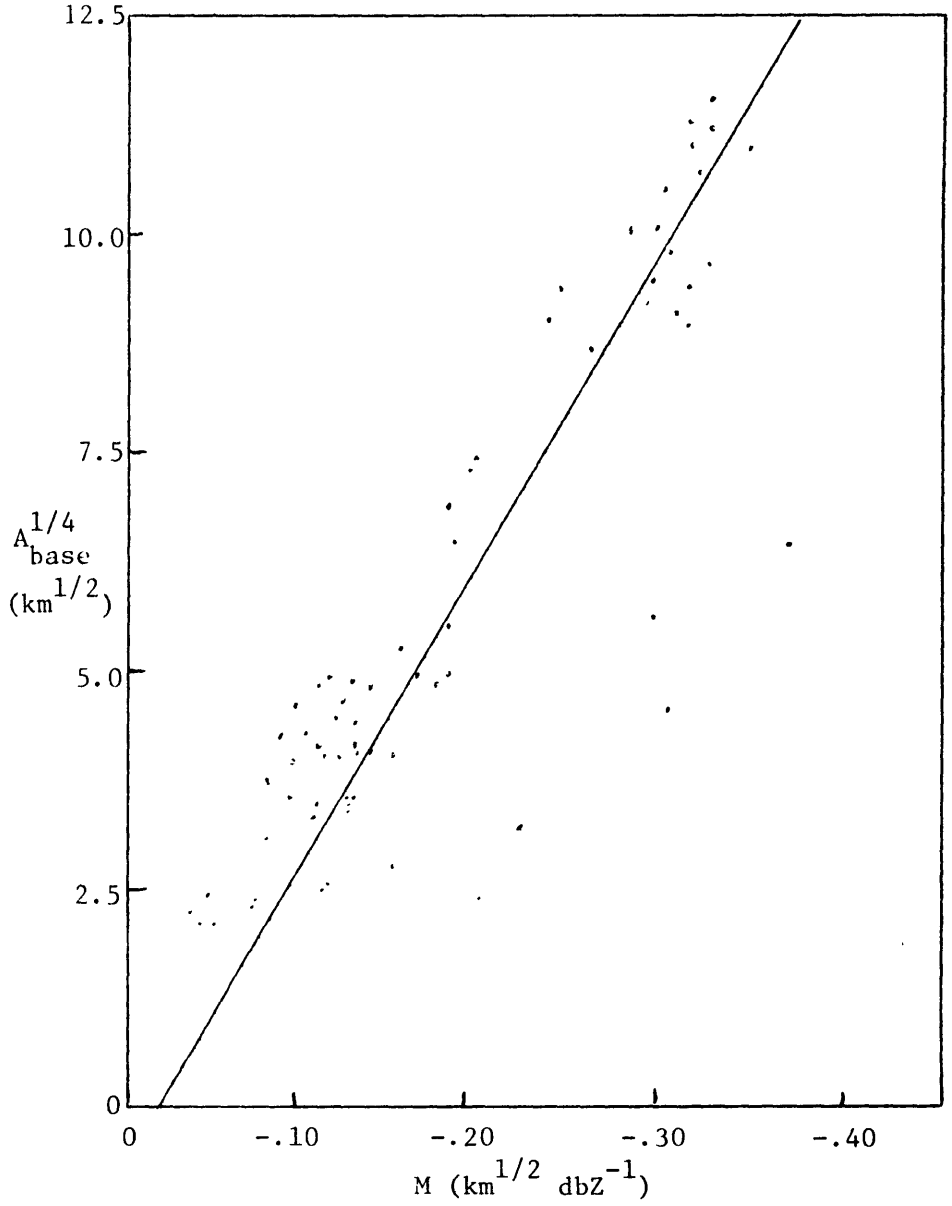

Figure 10. Scatter diagram used to determine prediction equation for M in the July squall line

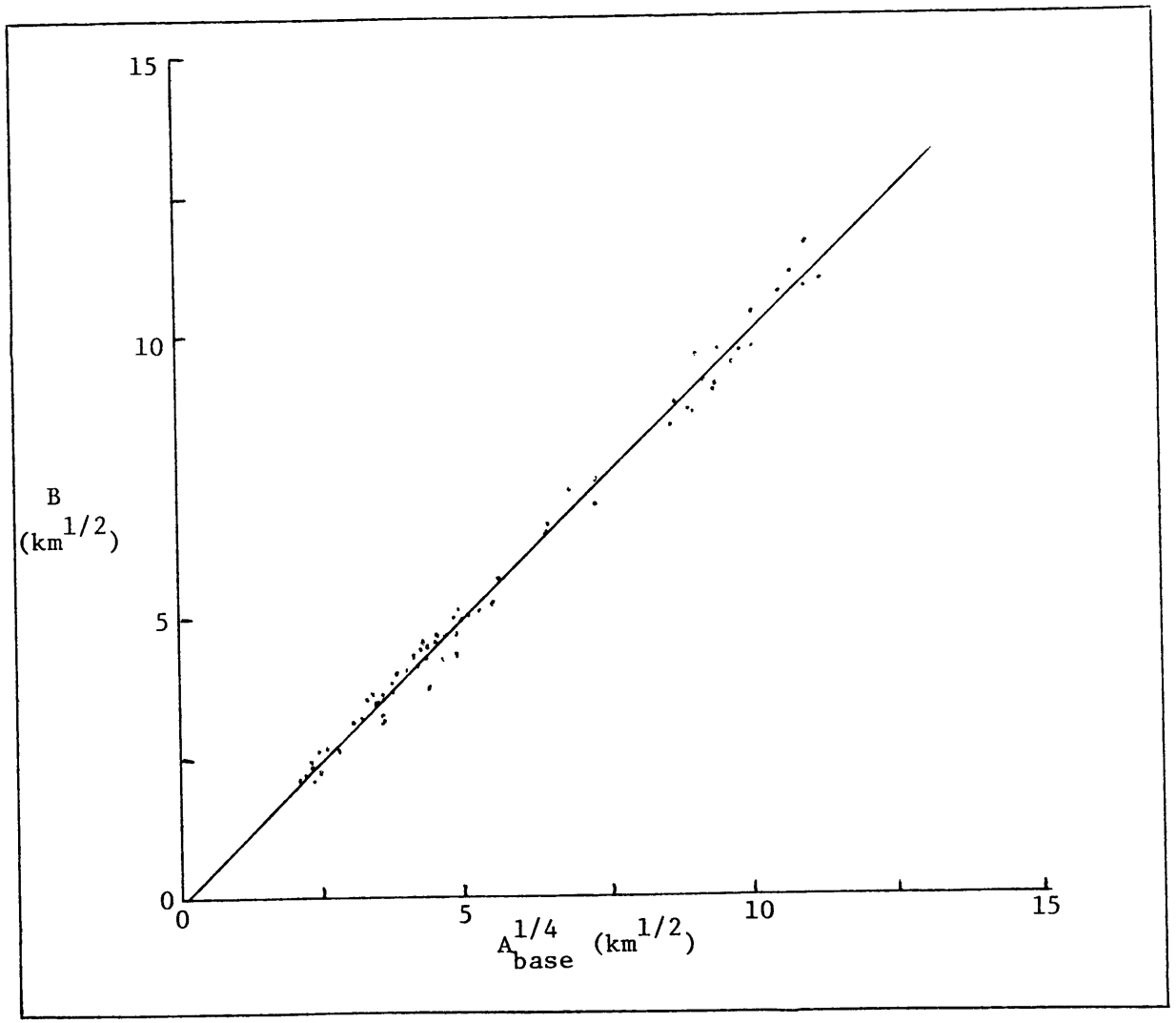

Figure 11. Scatter diagram used to determine the prediction equation for B in the July squall line

values obtained using $(A_Y)^{1/4} = MY + B$. Figure 12 shows the results for three of the areas considered. The dashed line represents the actual variation of areal coverage while the solid line was obtained by predicting M using the empirical relation with B given by $(A_{base})^{1/4}$. Although the fit was not always as good as indicated by these three areas, in general for the July squall line, the areal coverage at a given intensity value could be reasonably well approximated in terms of Y and the areal coverage at the base contour.

The same techniques were applied to the September '75 storm. For each of the largest five or six areas identified at 24 dbZ on each of the six maps available, the best fit line was determined to describe the areal coverage as a function of intensity. Once again, the slopes obtained for the thirty one areas were plotted against the fourth root of area covered at 24 dbZ on the scatter diagram shown in Figure 13. The best fit line to predict M in units of $km^{1/2}dbZ^{-1}$ was determined to be:

$$M = -.177 - .026(A_{base})^{1/4}$$

where the area is expressed in km^2. The scatter diagram shown in Figure 14 was constructed and the best prediction equation for B in units of $km^{1/2}$ was determined to be:

$$B = -.212 + 1.083(A_{base})^{1/4}$$

where the area is expressed in km^2. In this storm B was not as well approximated by the fourth root of the areal coverage at the base threshold, but the difference was less than 8%. Using the empirical formulae to predict M and B for use in the general equation

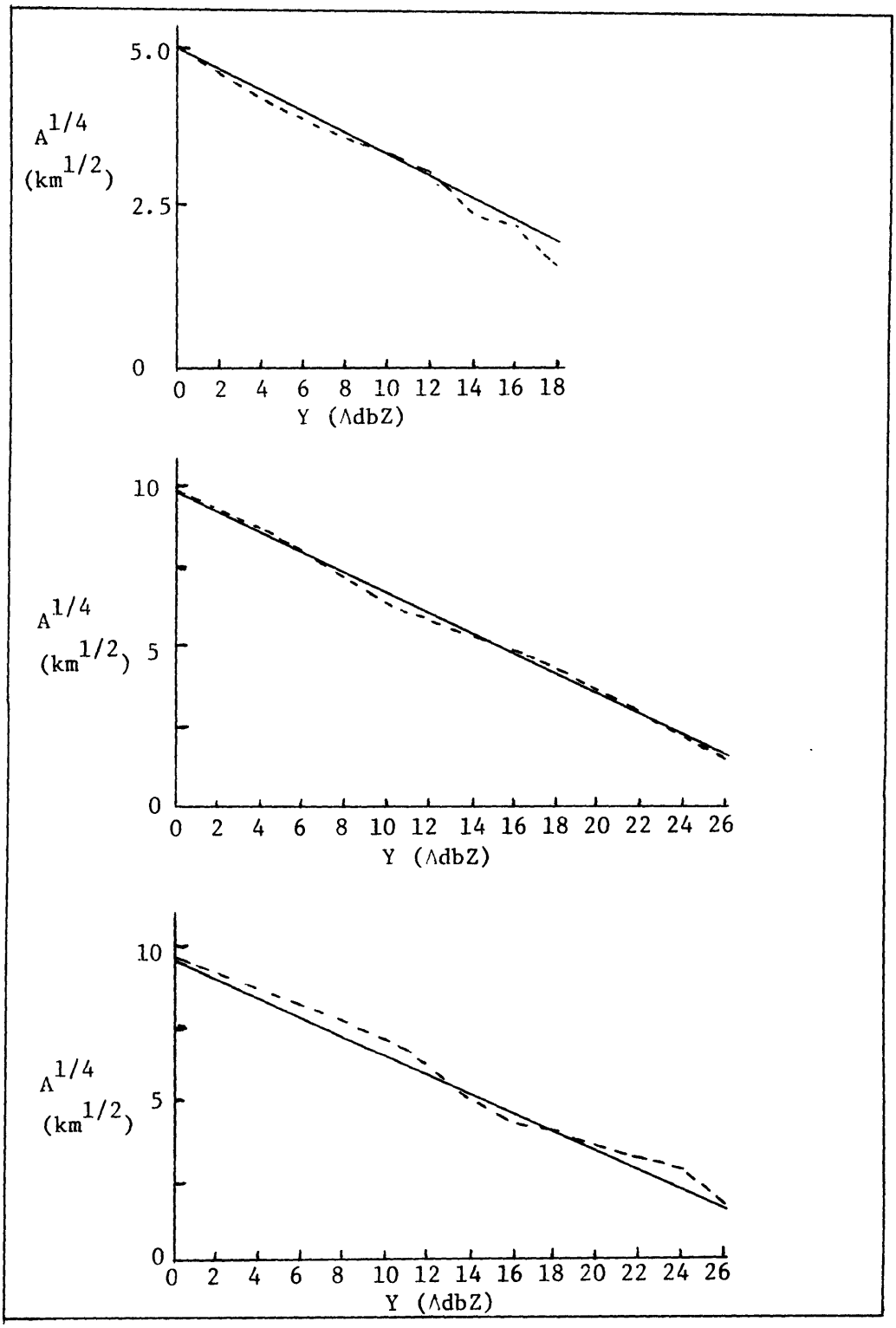

Figure 12. Actual (---) and predicted (——) distributions of area as a function of increment in intensity above 24 dbZ for three precipitation areas in the July squall line

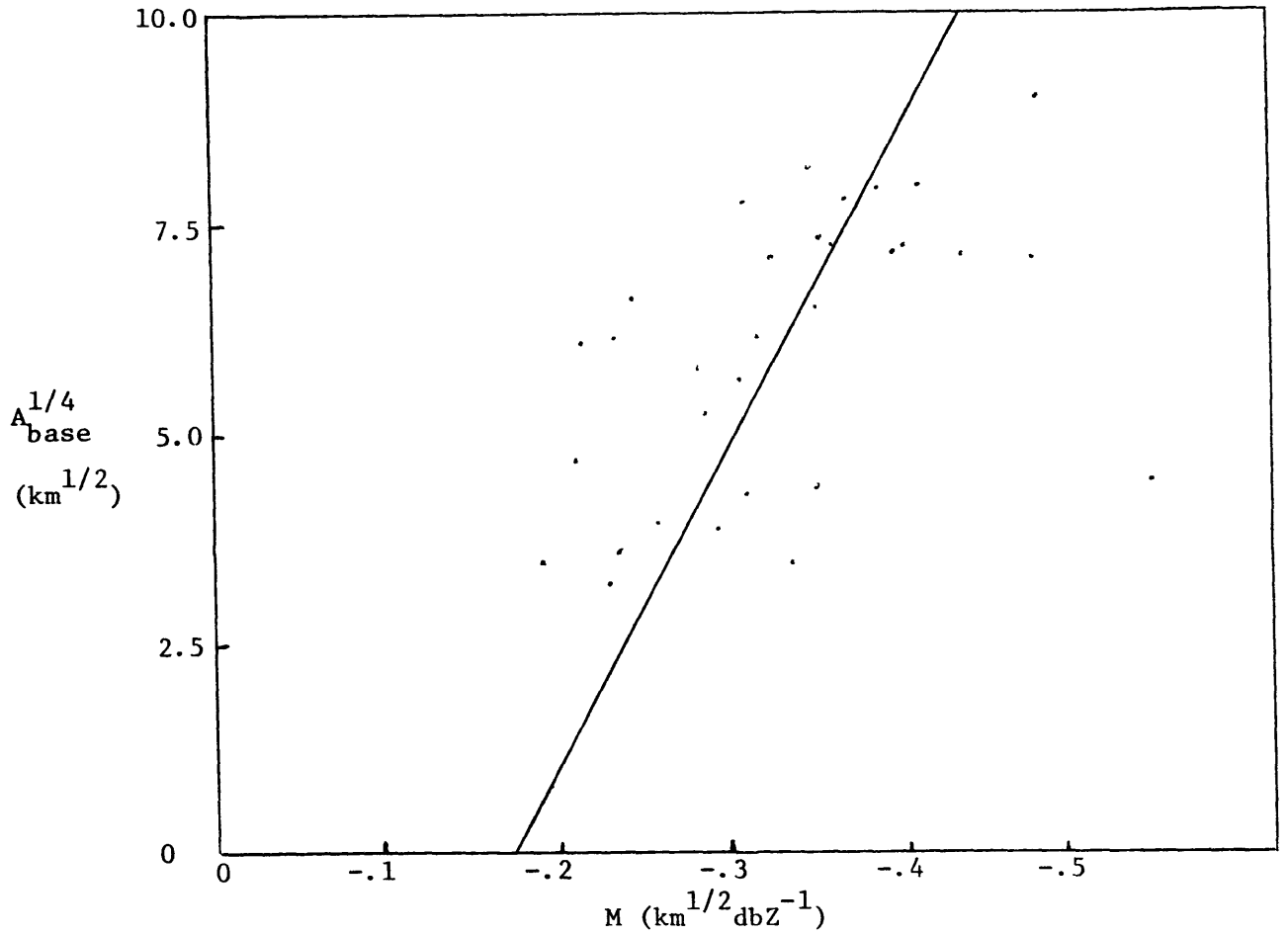

Figure 13. Scatter diagram used to determine the prediction equation for M in the September '75 storm

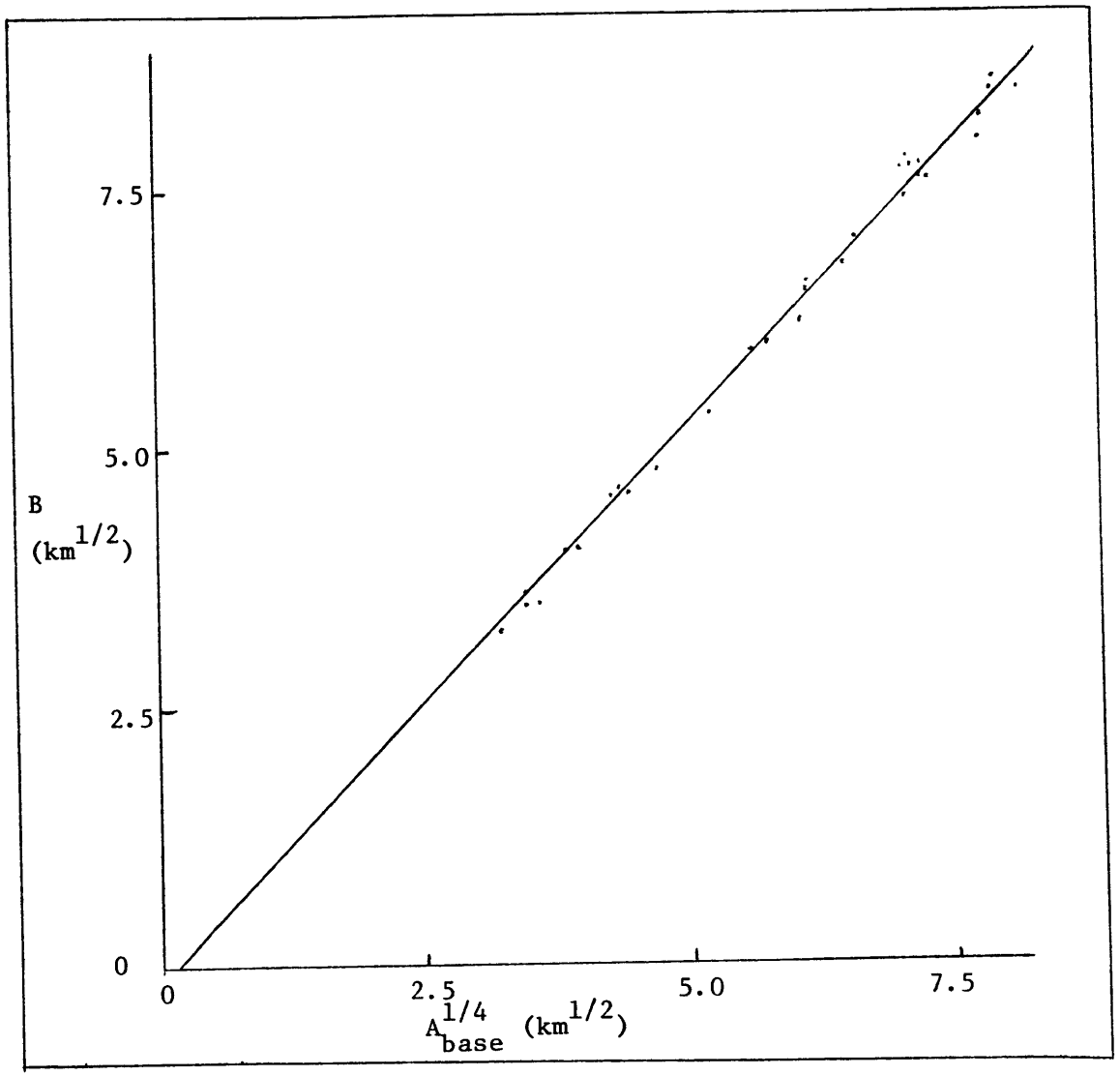

Figure 14. Scatter diagram used to determine the prediction equation for B in the September '75 storm

$(A_Y)^{1/4} = MY + B$ again yielded good results for individual areas in this storm as shown in Figure 15 where the dashed line is the observed distribution and the solid line represents the predicted distribution of area with intensity.

In both the July '75 and September '75 storms, it was possible to describe the distribution of area with intensity by means of empirical formulae which were based on the size of the areas under consideration. Combination of the relations presented above yielded the following expressions for the areal coverage at any intensity threshold:

$$(A_Y)^{1/4} = -.019Y + (1.009 - .03Y)(A_{base})^{1/4} - .088$$

for the July storm and

$$(A_Y)^{1/4} = -.177Y + (1.083 - .026Y)(A_{base})^{1/4} - .212$$

for the September storm where A_Y is the areal coverage in km^2 of precipitation of intensity at least Y dbZ above the threshold of 24 dbZ and A_{base} is the areal coverage in km^2 at 24 dbZ.

The relationship between the slope and the peak intensity of a given precipitation area was explored by constructing scatter diagrams of M against the peak intensity for both storms. The plots for both storms consisted of widely scattered points which exhibited no semblance of order. In both the July and September storms, any dependence of M on the peak intensity was much less significant than its dependence on areal size.

The relationship between the slope M and the areal coverage at the peak intensity for each area was also explored with a scatter

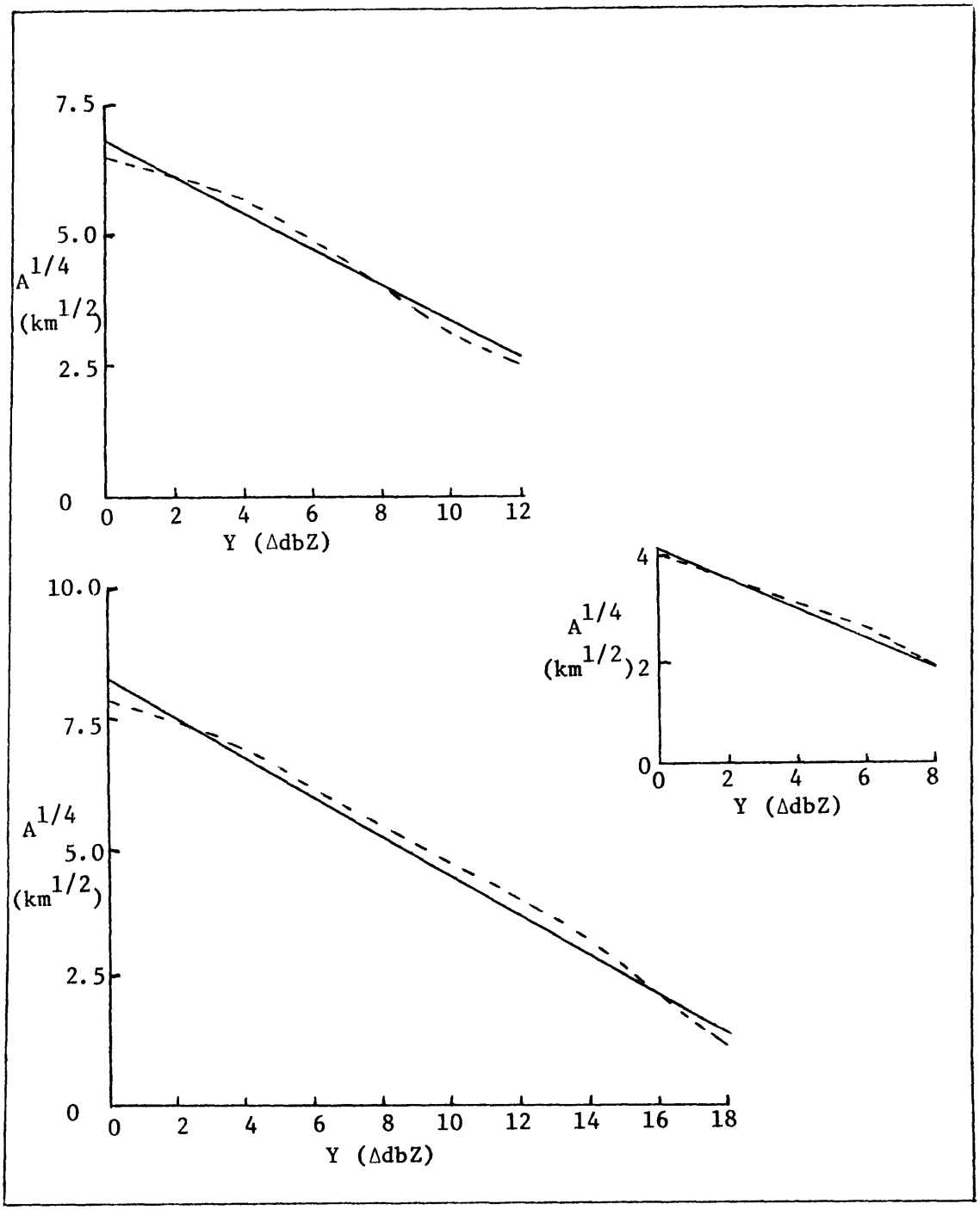

Figure 15. Actual (---) and predicted (——) distributions of area as a function of increment in intensity above 24 dbZ for three precipitation areas in the September '75 storm

diagram. Again, the wide disperson of points in the diagrams for both the July squall line and the September '75 storm prevented the determination of a relationship. This can partially be explained by considering the resolution of the radar. The intensity peaks generally covered only one or two points on a digital map. Therefore, there was little variation in the areal coverage of the peak intensity with most of the variation being caused by the fact that the peaks were located at different ranges during the radar coverage of the storm. For a 185km (100 n.m.) map with the first 20 range gates eliminated, the areal coverage associated with one point on a digital map varies from $1.2km^2$ at 37km to $7.1km^2$ at 220 km. For both storms this resolution accounted for practically all the variation in areal coverage of the peak intensity. As in the case of the peak intensity value for a given area, the influence on M of the areal coverage at the peak intensity was far less important than the area size.

Overall, it was observed that the fourth root of the area covered by precipitation in excess of a given intensity varied more or less linearly with the intensity both for entire maps and individual precipitation areas. Within a given storm, the slopes and intercepts of the lines describing the larger individual areas were linearly related to the size of the areas at 24 dbZ but the relationships differed between the two storms for which empirical prediction formulae were obtained. Therefore, these formulae cannot be used in a general prediction sense until more storms are studied and a general mode is worked out for determining these parameters from easily measurable

quantities.

E. THE RELATION BETWEEN SIZE AND INTENSITY

Since both size and intensity would seem to be important factors in determining significance of precipitation areas, a relation was sought between the two. Such a relation would indicate whether the largest areas are likely to contain the highest intensities. The procedure used was to plot the fourth root of the areal coverage of every area identified at a given base intensity against the peak Y value (Y_p) of the area. This was done using several intensity values as the base contour. In the July storm, all values from 24 to 42 dbZ were used as base values and in the September '75 storm, all values from 24 to 32 dbZ were used. At each base intensity threshold, the least squared fit first, second and third order curves to describe the data were determined. These forumlae were obtained to predict the size of an area as a function of the increment in intensity of the peak intensity of the area above the threshold intensity. These curves were then plotted and the lowest order formula which yielded a reasonable fit to the data points was selected for each threshold. Figure 16 shows an example of the scatter diagram and the three curves obtained for the 24 dbZ base threshold in the July storm. Figures 17 and 18 show the 36 dbZ and 40 dbZ base threshold diagrams for the July storm which were best described by the second (36 dbZ) and first (40 dbZ) order curves shown. Table 12 gives the equation selected for each base intensity threshold in both storms.

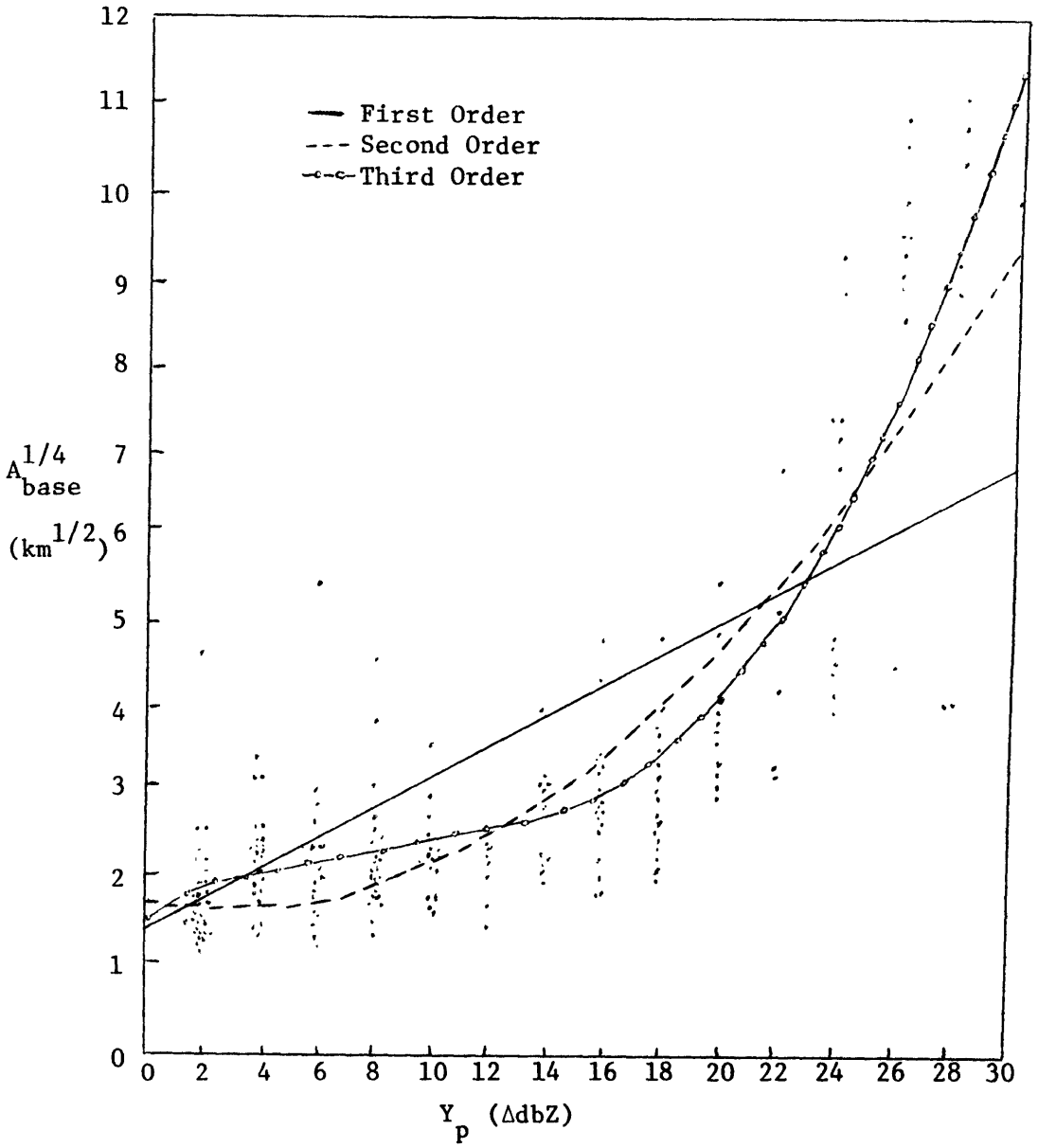

Figure 16. Best first, second, and third order curves to predict areal coverage at 24 dbZ as a function of peak intensity in the July squall line. In the figure, Y_p is the increment above 24 dbZ of the peak intensity

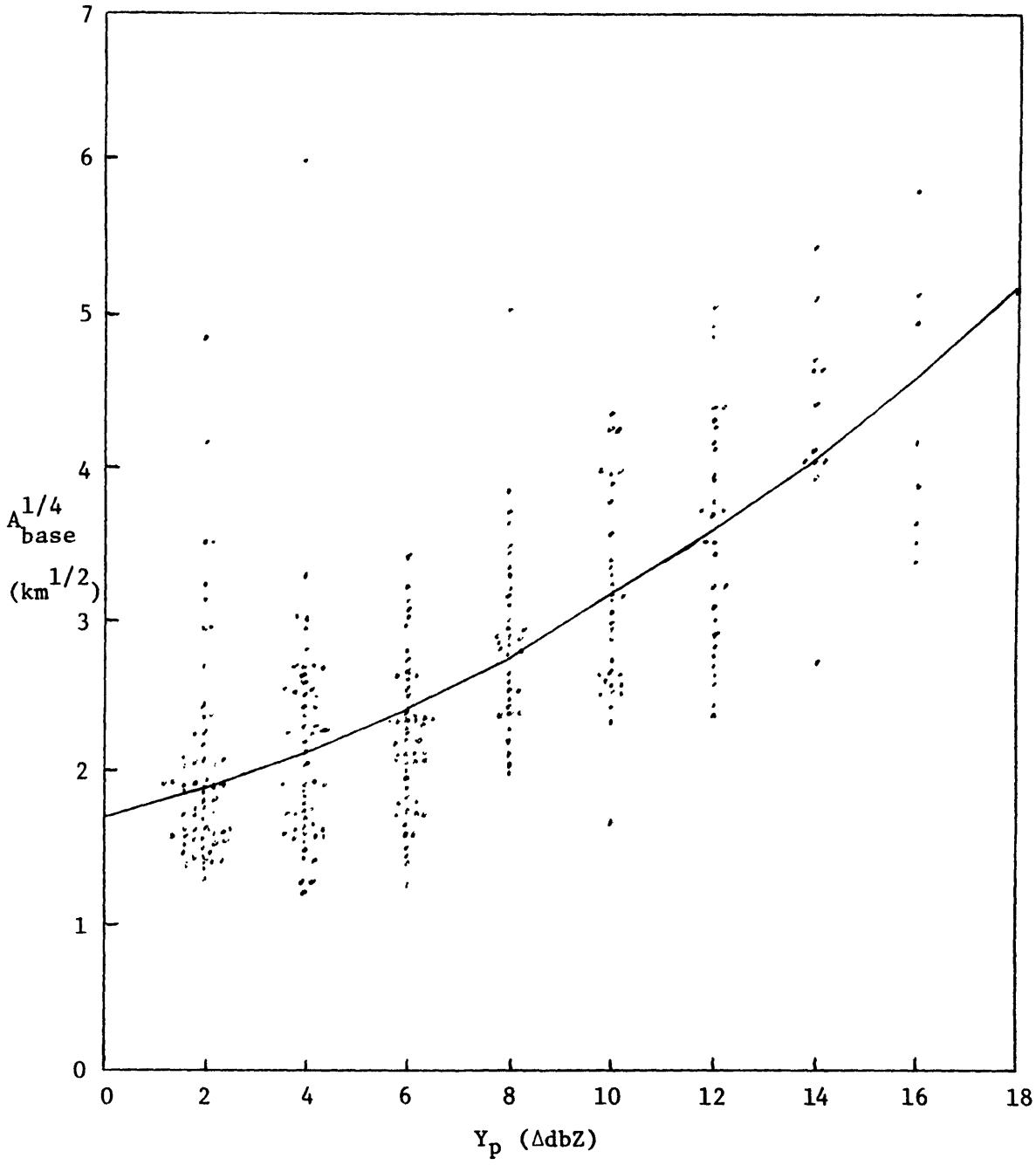

Figure 17. Scatter diagram used to determine equation to predict areal coverage at 36 dbZ as a function of peak intensity in the July squall line. In the figure, Y_p is the increment above 36 dbZ of the peak intensity and the relation is a seond order curve

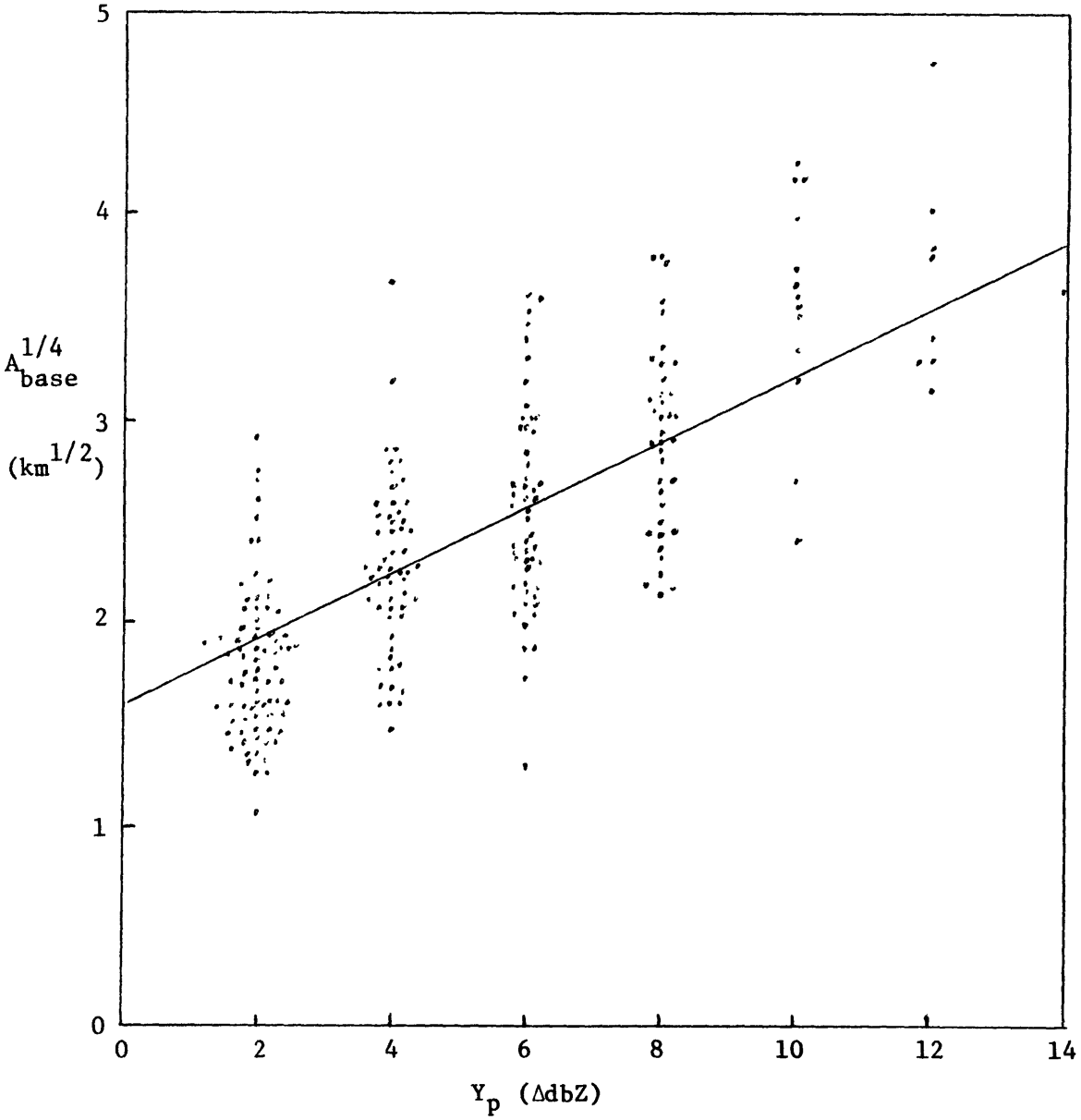

Figure 18. Scatter diagram used to determine equation to predict areal coverage at 40 dbZ as a function of peak intensity in the July squall line. In the figure, Y_p is the increment above 40 dbZ of the peak intensity and the relation shown is a linear one.

Table 12. Equations to predict size of an area at various thresholds (DBZ) as a function of the increment in intensity (Y_p) of the peak intensity of the area above the threshold

JULY STORM

	DBZ	EQUATION
I	24	$A_{base}^{1/4} = 1.688 + .162Y_p - .0159Y_p^2 + .0007153Y_p^3$
	26	$A_{base}^{1/4} = 1.675 + .1742Y_p - .01729Y_p^2 + .0007955Y_p^3$
	28	$A_{base}^{1/4} = 1.688 + .1566Y_p - .01457Y_p^2 + .0007629Y_p^3$
	30	$A_{base}^{1/4} = 1.688 + .1925Y_p - .01838Y_p^2 + .0009252Y_p^3$
II	32	$A_{base}^{1/4} = 1.743 + .07426Y_p + .004940Y_p^2$
	34	$A_{base}^{1/4} = 1.688 + .09474Y_p + .004281Y_p^2$
	36	$A_{base}^{1/4} = 1.688 + .08524Y_p + .005982Y_p^2$
	38	$A_{base}^{1/4} = 1.593 + .1134Y_p + .005475Y_p^2$
III	40	$A_{base}^{1/4} = 1.593 + .1624Y_p$
	42	$A_{base}^{1/4} = 1.552 + .1838Y_p$

SEPTEMBER STORM

	DBZ	EQUATION
I	24	$A_{base}^{1/4} = 1.777 + .2103Y_p + .001005Y_p^2 + .0008691Y_p^3$
II	26	$A_{base}^{1/4} = 1.634 + .2230Y_p + .01538Y_p^2$
	28	$A_{base}^{1/4} = 1.576 + .2986Y_p + .01504Y_p^2$
	30	$A_{base}^{1/4} = 1.634 + .4001Y_p + .0104Y_p^2$
III	32	$A_{base}^{1/4} = 1.691 + .4719Y_p$

In both storms, the curves fell into three groups. For the lower intensity thresholds, the best curves were the third order curves. The middle range base intensity data were well described by a second order curve and the higher base intensity data were best described by a linear relation. Within each storm, the overall trend was for the equations to become more linear as the threshold value increased.

A point of interest is that the coefficient of Y_p^2 was negative in all the Group I equations in the July storm and positive for Group I in the September storm. The effect was to keep the curves flatter over a wider range of intensity in the July storm. The large areas in the July storm were observed to contain rather high peak intensities while the highest intensity observed in the September storm was 44 dbZ. Therefore, since the large areas identified at the lower intensity thresholds were the same order of magnitude in terms of size in both storms, the curves grew more rapidly at the lower values of Y_p in the September storm than in the July storm. This same effect is responsible for the overall trend toward larger coefficients in the September storm.

In general, both storms indicated a strong tendency for the larger areas to also be the most intense. The relationship between size and intensity was strong enough to allow the determination of empirical formulae to predict the size of an area as a function of its peak intensity. Again, the prediction equations differed for the two storms which were considered. Consequently, before such formulae can be used in general, many more storms will have to be analyzed to

determine the most representative prediction equations.

F. THE SIGNIFICANCE OF AREAS

As was indicated earlier, both the large number and wide range of sizes of areas found at nearly all intensity thresholds pointed out the need for some method of selecting the areas of interest for a particular study or application. A mesoscale precipitation area would be assumed to be significant if it represented a region of relatively intense precipitation which retained its identity over some period of time. However, for a single map, the retention of identity with time cannot be determined and a measure of significance would presumably have to be based on such characteristics as size and intensity.

The question of which areas at a particular intensity threshold are significant and which are not is complicated not only by the different characteristics of the individual areas but also by three particular situations which can occur in the data. Figure 19 illustrates these situations. The first situation (a) is one which occurs when several separate areas are identified by an intensity threshold when in reality the several areas are physically one concentration of precipitation. In this situation, the several areas may be considered individually insignificant while if they were considered one area, it could be found to be significant. The opposite situation is portrayed in (b) where one significant area could be found because of a narrow connection between what physically appears to be two possibly

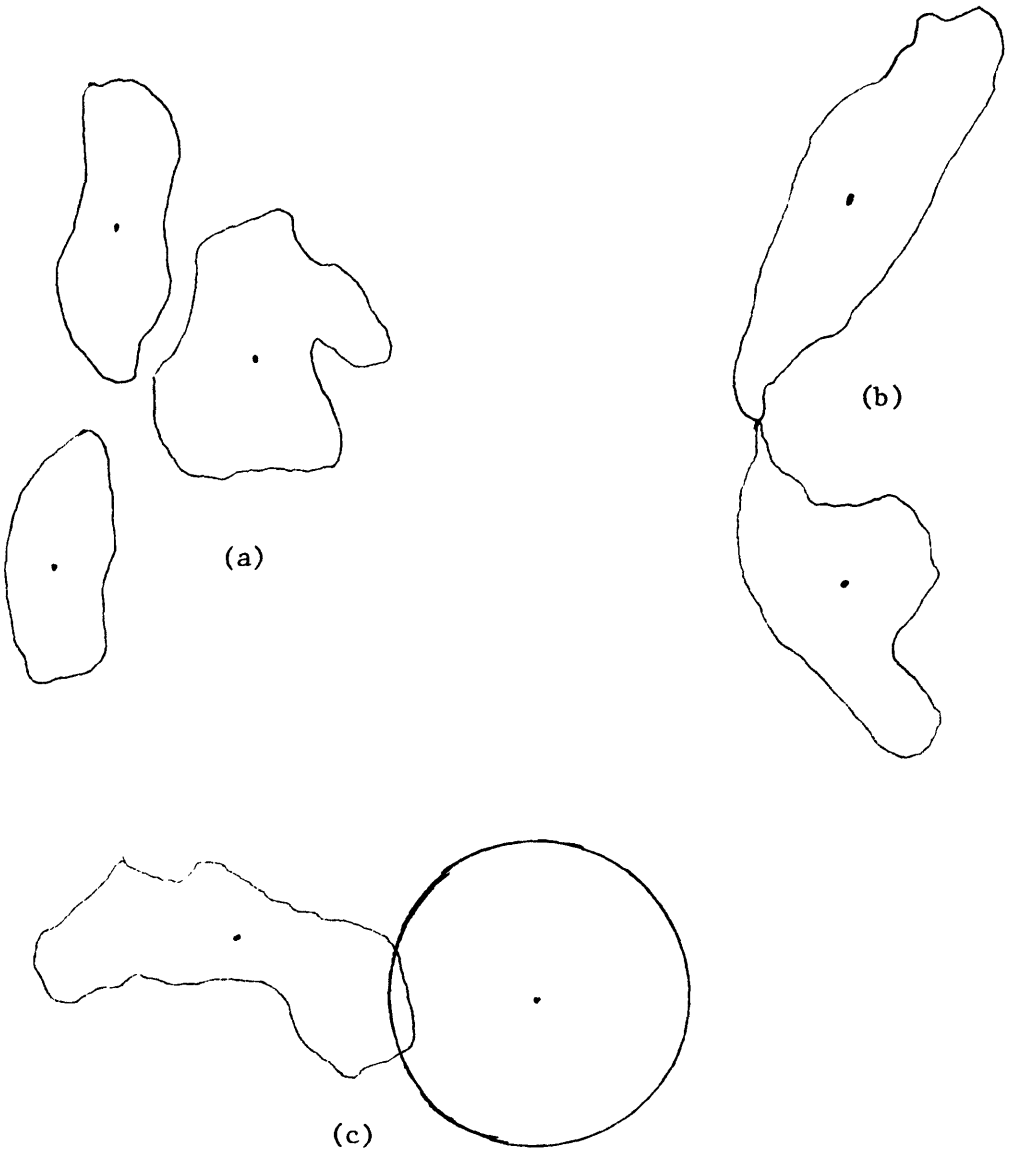

Figure 19. Illustrations of three situations which complicate the problem of significance of areas

insignificant areas. The final situation (c) is caused by the inability of the radar to view an entire precipitation area as it moves into range. The small area discerned by the radar may be deemed insignificant although it could be the edge of a highly significant area. The first problem (a) is very similar to the signal breakthrough phenomenon except on a larger scale. A possible solution would be to consider areas whose centroids were within some distance of each other as one area. The critical distance would have to be a function of areal size. The second situation (b) is more difficult to handle since only one area has been identified. One possible solution would be to introduce into the centroid program both azimuthal and radial checks to see if the dimension of the area under consideration fell below some critical limit. If so, then the area could be terminated and a new area formed beyond the narrow connection.

These three situations also introduce biases into the analyses of the number of areas and their sizes. However, the effect on these two analyses is qualitatively not as great as the importance which the situations hold for the significance problem. The situations portray rather large areas and we have seen that the number of large areas is rather small at all thresholds. Therefore, whether one area of $10^3 km^2$ was detected or 2 areas of $500 km^2$ were found would have very little influence on the analyses of observed sizes and numbers. However, since a measure of significance should include a consideration of size as well as intensity, the problem introduced by such occurrences is very real. A qualitative look at the data seemed to indicate

these situations were not very common, but their existence must be recognized.

With the assumption that the situations described above do not occur often enough to be overly important, the problem of significance is basically the determination of appropriate criteria which will eliminate the many unimportant areas which exist at all thresholds. No breakpoint could be found in the data during the course of this study which would serve as a natural significance criterion and it is doubtful that a criterion could be found that would be suitable for all types of studies or applications. Therefore, any criterion which suited the purpose at hand would be an appropriate one.

The criterion selected for this study was to choose the 5 largest areas at a given intensity threshold as being the most significant. Presumably a more appropriate criterion would be based on both size and intensity. However, the strong relationship observed between size and intensity indicates that some measure of intensity is included in a size criterion. This lends support to the choice of selecting the 5 largest areas in the determination of the empirical prediction formulae for M and B and in testing the acceptability of the sizes of areas defined by the 30 and 36-38 dbZ thresholds. As a further test of this criterion, the percentage of the total area covered by precipitation of at least 24, 30 and 36-38 dbZ intensity which was contained in the 5 largest areas was determined for each map. The result was that the 5 largest areas contained an average of 94% of the total coverage at 24 dbZ. At 30 dbZ, the average was 84% and

at 36-38 dbZ, the average was 77%. Although a decrease was observed with increasing intensity, even the lowest vlaue of 77% indicated that more than three-fourths of the precipitation was contained in the 5 largest areas. For the purposes of this study then the choice of the 5 largest areas as being the significant ones was quite satisfactory.

Another criterion which could be used would be to select areas in excess of a predetermined size threshold as being significant. With the selection of the 5 largest areas, it would be possible to include some rather small areas as being significant if most of the precipitation was contained in one or two very large areas. This would be avoided by using a size threshold as the significance criterion. However, the selection of an appropriate size threshold for each intensity level would be a difficult task.

Still another significance criterion could be to select at each intensity threshold as many areas as would be necessary in order to include a predetermined percentage of the total area covered by precipitation of at least the intensity in question. This would be accomplished by selecting areas starting with the largest one and working down until the desired percentage coverage was obtained.

There is no reason to assume any one of these criteria would be more appropriate than the others. Since no natural criterion could be determined from extensive examination of data, presumably an appropriate significance criterion must be selected for each study or application in view of its purpose. For any given study such a criterion could be defined in terms of size, intensity or both.

V. CONCLUSIONS AND APPLICATIONS

A. SUMMARY OF RESULTS

Perhaps the most definitive statement that can be made at the conclusion of this study is that the precipitation patterns revealed by the high-resolution digital data are far more complex than could be realized by using quantized PPI displays. The fact that upwards of 40 separate identifiable areas could be found at several different intensity thresholds on a map of a relatively well organized squall line is an excellent indication of the degree of complexity involved. The details revealed in the complex patterns are sometimes more of a hindrance than a help in analysis procedures and often make the desire for the high degree of intensity resolution available with digital data a questionable one. Nonetheless, the details do indicate that it is not possible to describe the intricate precipitation patterns which exist by a simple formulation and that any attempt to describe patterns must be on a scale which encompasses an overall picture and smooths the unimporatnt details.

Two main areas of study were undertaken with this highly complex digital data base. First, an attempt was made to find intensity thresholds which could be used to help identify the mesoscale precipitation features called large mesoscale areas (LMSA's) and small mesoscale areas (SMSA's) which had been defined and studied by Austin and Houze (1972) and Reed (1972). Second, characteristics of precipitation areas such as the distribution of areal coverage with intensity and the relation between size and intensity were sought.

Such characteristics would not only serve to increase the understanding of precipitation patterns but also could have application to the modeling of storms.

The first technique employed to find intensity thresholds which would identify mesoscale areas was to search for natural breaks in the distribution of total areal coverage as a function of intensity. Such breaks would indicate which intensity thresholds showed small changes in areal coverage and therefore define transitions between different sized mesoscale phenomena. The observed distributions however were very well behaved with no distinct kinks or breaks. In an attempt to break this apparent continuum in the distribution of the total areal coverage with intensity, intensity thresholds were sought at which significant merging of several smaller areas into a few larger areas took place. Conceptually, such thresholds would indicate transitions between large and small mesoscale areas or between small mesoscale areas and cells.

To identify the thresholds at which significant merging occurred, a detailed analysis of the behavior of the distribution of the number of areas existing as a function of intensity was undertaken. As a result, the overall picture of how the number of areas varies with intensity threshold appears to be fairly well determined. At the higher threshold values, only a few areas exist. As the threshold decreases, two effects operate simultaneously and oppose one another. The first effect is that more and more new areas appear causing a rapid rise in the total number of areas. The second effect is that of

merging areas which tends to decrease the total number of areas and serves to slow the rapid rate of increase in number which was observed at the higher intensities. The merging effect becomes increasingly important with decreasing intensity and actually becomes dominant at some thresholds resulting in a peak in the distribution of the number of areas with intensity. The one threshold region which consistently showed a peak regardless of the character or intensity of the different storms was in the vicinity of 30 dbZ. A minor secondary peak was observed between 38 and 42 dbZ in the intense July '75 squall line.

The distribution of sizes of precipitation areas as a function of intensity was examined to see if the preferred areal size showed distinct jumps at certain intensity thresholds. Such jumps would indicate significant merging and therefore important thresholds which could be used to define mesoscale areas. Histogramming the areas at each intensity threshold according to size indicated that the tendency at all intensities was for smaller areas to be by far the most numerous with the preferred size range rarely exceeding the 7-28km^2 interval.

Further use of the areal sizes was made through examination of a parameter F_N defined by

$$F_N = \left(\frac{1}{\text{number of areas}} \right) \ln \left(\frac{\text{maximum areal size}}{\text{mean areal size}} \right)$$

for each intensity threshold. At intensities where merging was important, the maximum areal size observed would increase and the number of areas would either remain about the same or decrease tending

to yield a peak in the distribution of F_N. Peaks were consistently observed near both ends of the intensity spectrum in all storms because of the relatively small number of areas. Usually one and occasionally two medium range peaks were observed in F_N in the middle to upper 30's with the more popular values being in the 36-38 dbZ range. At these intensities, merging was an important process although it was not often important enough to produce a peak in the distribution of the number of areas.

These techniques indicated that the thresholds in the vicinity of 30 dbZ and 36-38 dbZ held more importance than others with respect to merging. Conceptually, they could be used to identify LMSA's and SMSA's, respectively. It is hoped that the features identified by these thresholds are the same features which have been identified by previous investigators as mesoscale areas. The average size of the larger areas identified at these thresholds were of the proper order of magnitude to lend support to the contention that the features are the same. However, only analysis of these areas in time sequences will provide the final conclusion.

The most applicable results of this study concerned the characteristics of precipitation areas. It was observed that for a map as a whole, as well as for individual precipitation areas, the fourth root of the areal coverage at any intensity could be approximated as a linear function of the increment in dbZ above the base threshold intensity which was used to define the areas. That is,

$$(A_Y)^{1/4} = MY + B$$

where $Y = dbZ - dbZ_{base}$, M is the slope, and B is the intercept. This relation held in detailed analyses of both a cyclonic storm and a squall line. However, the constants M and B which yielded the best approximations for individual areas were highly variable from one area to another. Although the constant B for the linear approximation was not exactly the fourth root of the areal coverage, the difference was less than 8% for the cyclonic storm and less than 1% for the squall line. A very strong relation was observed between the areal size and M while virtually no relation could be found between M and the peak intensity or areal coverage at the peak intensity for a given precipitation area. Empirical prediction equations were obtained for M and B as a function of areal size for the threshold intensity of 24 dbZ in both storms.

The relations obtained to predict the areal coverage at any intensity for the two storms are shown below:

Squall Line

$$(A_Y)^{1/4} = - .019Y + (1.009 - .03Y)(A_{base})^{1/4} - .088$$

Cyclonic Storm

$$(A_Y)^{1/4} = - .177Y + (1.083 - .026Y)(A_{base})^{1/4} - .212$$

where A_{base} is the areal coverage at 24 dbZ expressed in km^2, and Y is the increment in dbZ above 24 dbZ of the intensity threshold whose areal coverage is being predicted (A_Y in km^2). These equations are noticeably different for each storm and although they yielded good results for the two storms which were considered, only further research will indicate if they would be valid for other cyclonic storms

or squall lines.

Individual precipitation areas were further analyzed to determine if a relation existed between size and intensity. In both the cyclonic and squall line storms, a strong relation between size and intensity was observed with the larger areas containing the highest peak intensities in all cases. For each storm, several threshold intensities were used as base contours and empirical equations were obtained to predict the areal size at the base contour as a function of the peak intensity of the area. In both storms, the best relation obtained for the lower base intensity thresholds was a third order relation with the best fit relation becoming more and more linear with increasing base intensity threshold. The equations obtained for the different base intensity thresholds considered in both storms are given in Table 12. These equations are quite different for each storm and therefore will not be useful in a general prediction sense until many more storms are examined. However, they <u>are</u> useful simply to point out that a relationship exists between size and intensity.

This strong relationship between size and intensity has a direct bearing on the question of which precipitation areas at a given threshold intensity are significant and which are trivial. Since no natural criterion could be found, the approach used in this study was to consider the 5 largest areas at a particular intensity threshold as the most significant ones. It was observed that an average of 94% of the total area covered on a given digital map by precipitation of at least 24 dbZ intensity was contained in the 5 largest areas. The

same average for the 30 and 36-38 dbZ thresholds was found to be 84% and 77% respectively. These high percentages and the strong relationship observed between size and intensity both lend support to the validity of the significance criterion selected. An equally acceptable choice would be to consider the areas in excess of a predetermined size threshold as being the most significant at a given threshold intensity. Because it is unlikely that any general significance criterion could be found which would be suitable in all cases, it is concluded that the significance criterion must be determined by the purpose at hand and any reasonable one would be acceptable.

B. APPLICATON OF RESULTS

Although this study did not point out exact intensity thresholds which could be used to identify mesoscale precipitation areas, the results indicate that thresholds in the vicinity of 30 dbZ and 36-38 dbZ are more likely candidates than others. These threshold regions are ones at which significant meshing of several small areas of precipitation into larger more important areas occurs. Also, the sizes of the larger areas defined by these threshold regions are the proper order of magnitude for them to be considered large and small mesoscale areas as defined by Austin and Houze (1972). Therefore, these threshold regions can be considered general guidelines which could be followed to identify mesoscale areas for the purpose of examining their life histories.

The most applicable results of this study are based upon the

hypothesis concerning the relation between areal coverage and the increment in intensity above the defining threshold. Although the constants M and B for use in the relation $(A_Y)^{1/4} = MY + B$ were determined only for the 24 dbZ threshold in this study, they could be determined for higher intensity thresholds since it was observed that areas defined by the 30 dbZ threshold exhibited the same degree of linearity as those defined by 24 dbZ. Once these constants have been determined for higher thresholds, one could then describe the distribution of area with intensity within an LMSA or SMSA simply by measuring the size of the area at the defining threshold intensity. An alternative method would be to predict the area size at a given threshold intensity by measuring the peak intensity of the area and using the appropriate equation from Table 12 which gives relations between areal size at various thresholds and peak intensity.

Having described the distribution of area with intensity for a given precipitation area using the linear relation described above, one could then perform an integration and obtain the average intensity for the area. Also, the areal contribution of a given intensity value could be determined by direct integration. Using the rainfall rate associated with that particular intensity value, one could then determine the contribution to the total rainfall of precipitation of a particular intensity.

The empirical relations formulated in this study could be considered the groundwork to a storm model for use in hydrological studies. It is in this context that the results of this study appear to have

the most application.

C. SUGGESTIONS FOR FUTURE STUDY

This study has provided only preliminary results in the analysis of mesoscale areas. The full analysis procedures of this study should be employed in studies of other storms to see if the numbers and sizes of areas would be distributed similarly. Such detailed analysis procedures would also serve to determine more definitely whether a natural breakpoint exists which could be used as a significance criterion to eliminate unimportant areas at a given intensity threshold. The results of this study suggested that such breaks do not exist naturally.

Using intensity thresholds around 30 dbZ and 36-38 dbZ and applying appropriate significance criteria to delineate the important areas, one could undertake a study of the characteristics of LMSA's and SMSA's. Such studies should include analysis of the vertical structure of the mesoscale areas as depicted by the three dimensional digital radar maps. Also, analysis of such areas in time should be undertaken to determine how the characteristics of the areas vary throughout their lifetimes. Such studies will be essential to the ultimate understanding of the meteorological processes involved in this scale of activity.

A major area of research which could be undertaken is the development of a model of mesoscale precipitation areas for use in hydrology. As a first step in this direction, the validity of the

linear distribution of the fourth root of area as a function of intensity should be tested in a much larger sample of storms. Also, empirical prediction formulae for M and B should be established for several different intensity thresholds in storms of different character to see if general reliable prediction equations can be found or if it will be necessary to stratify prediction formulae according to such parameters as storm type, storm intensity, or season. In addition to the determination of such formulae, the spatial distribution of intensity would have to be studied in order to completely describe the areas. However, the usefulness of such a model would be well worth the effort of development.

ACKNOWLEDGEMENTS

I express my appreciation to the United States Air Force Institute of Technology for making possible my study at MIT.

Special appreciation is due Dr. Pauline M. Austin whose assistance during the conduct of this study was invaluable.

I would like to express sincere thanks to my wife, Ann, who not only typed all the drafts and the final manuscript, but also was very understanding and provided much encouragment while the research was underway.

To Captain Gerald F. Riley, I express thanks for the assistance provided by hours of discussion on the many problems encountered during the study.

BIBLIOGRAPHY

Austin, P. M., 1960: Microstructure of Storms as Described by Quantitative Radar Data. Physics of Precipitation, Geophysical Monograph No. 5, NAS-NRC No. 746, American Geophysical Union, pp. 86-92.

Austin, P. M., and R. A. Houze, Jr., 1972: Analysis of the Structure of Precipitation Patterns in New England. Journal of Applied Meteorology, 11, pp. 926-935.

Austin, P. M., and C. Morrow, 1975: Unpublished result of research conducted on the Weather Radar Project at the Massachusetts Institute of Technology, Cambridge, Massachusetts.

Blackmer, R. H., Jr., and R. O. Duda, 1972: Application of Pattern Recognition Techniques to Digitized Radar Data. Final Report, Contract 1-36072, SRI Project 1287, Stanford Research Institute, Menlo Park, California.

Browning, K. A., and T. W. Harrold, 1969: Air Motion and Precipitation Growth in a Wave Depression. Quarterly Journal of the Royal Meteorological Society, 95, pp. 288-309.

Elliott, R. D., and E. L. Hovind, 1964: On Convective Bands Within Pacific Coast Storms and Their Relationship to Storm Structure. Journal of Applied Meteorology, 3, pp. 143-154.

Johnson, G. N., P. L. Smith, Jr., F. E. Nathanson, and L. W. Brooks, 1975: A Study of Techniques for Reduction of Anomalous Propagation Problems in Weather Radar Data Systems. Report 75-2, Contract 4-35341, Institute of Atmospheric Sciences, South Dakota School of Mines and Technology, Rapid City, South Dakota.

Ostlund, S. S., 1974: Computer Software for Rainfall Analyses and Echo Tracking of Digitized Radar Data. NOAA Technical Memorandum ERL WMPO-15.

Reed, R. W., 1972: Characteristics and Development of Mesoscale Precipitation Areas in Extra-Tropical Cyclones. S. M. Thesis, Department of Meteorology, MIT.

Schaffner, M. R., 1975: On the Characterization of Weather Radar Echoes. Procedures of the 16th Weather Radar Conference, April, 1975, Houston, Texas.

Wiggert, V., and G. F. Andrews, 1974: Digitizing, Recording, and Computer Processing Weather Radar Data at the Experimental Meteorology Laboratory. NOAA Technical Memorandum ERL WMPO-17.

APPENDIX I

Provided on the following pages is a copy of the FORTRAN computer program named the Centroid Program. This program accepts digital radar maps in polar coordinates in punch card form and outputs area-weighted centroids in polar coordinates as well as area size in square nautical miles for precipitation areas identified at every intensity threshold from the peak intensity on the map down to 20 dbZ in increments of 2 dbZ.

```
C      THIS PROGRAM DETERMINES CENTROIDS FOR PRECIPITATION AREAS ABOVE
C      A GIVEN THRESHOLD DBZ VALUE WITH 20 NM OF GROUND CLUTTER ELIMINATED
       DIMENSION SUMR(300),SUMZ(300),SUMT(300),AREA(100),RANGE(100)
       INTEGER*2 IPB(300,361),IPE(300,361),IMA(99),IBEG(361,20),IEND(361
      A,20),I(361),A(361,100),AZAR(361)
       ICARD=5
       IPRINT=6
C       READ IN IXMAX(NO. OF RANGE BINS), IMAXR(NO. OF RAYS), NRGS
C      (NO. OF RANGE GATES SKIPPED), AND R(RANGE IN NM)
       READ(ICARD,1001) IXMAX,IMAXR,NRGS,R
C      LOAD THE DBZ MAP INTO THE A ARRAY AND THE AZIMUTHS INTO AZAR
       DO 8 IY=1,IMAXR
       READ(ICARD,1002) IAZ
       READ(ICARD,1003) (A(IY,IX),IX=1,IXMAX)
8      AZAR(IY)=IAZ
C      THIS SEGMENT PRINTS A HARD COPY OF THE MAP AND WORKS ONLY FOR MAPS
C      HAVING 100 RANGE BINS
       WRITE(IPRINT,7008)(AZAR(IY),(A(IY,IX),IX=1,40),IY=1,IMAXR)
       WRITE(IPRINT,7008)(AZAR(IY),(A(IY,IX),IX=39,78),IY=1,IMAXR)
       WRITE(IPRINT,7009)(AZAR(IY),(A(IY,IX),IX=76,100),IY=1,IMAXR)
C      IYMIN IS THE FIRST AZIMUTH AND IYMAX THE LAST
       IYMIN=1
       IYMAX=IMAXR
       IDBZM=0
       RSTEP=R/FLOAT(IXMAX)
       AFACT=RSTEP*0.0174532
       R1=RSTEP*FLOAT(NRGS)
       RP=R1
       WRITE(IPRINT,7005)
       WRITE(IPRINT,7006) R,NRGS,RSTEP,AFACT
C      LOAD THE AREA AND RANGE ARRAYS
       DO 866 IB=1,IXMAX
       AREA(IB)=RP*AFACT
       RANGE(IB)=RP
866    RP=RP+RSTEP
```

```
      WRITE(IPRINT,7004)
      WRITE(IPRINT,7003) (AREA(IB),IB=1,IXMAX)
C     THIS SECTION ELIMINATES 20 NM OF GROUND CLUTTER
      IF(R1-20.0) 404,403,403
404   IF(R-100.0) 406,401,402
406   IGT=41-NRGS
      GO TO 405
401   IGT=20-NRGS
      GO TO 405
402   IGT=10-NRGS
405   DO 407 IGL=1,IGT
      DO 407 IY=1,IMAXR
407   A(IY,IGL)=0
403   CONTINUE
C     FIND THE MAXIMUM DBZ VALUE ON THE MAP
      DO 7 IY=1,IMAXR
      DO 7 IX=1,IXMAX
7     IF(A(IY,IX).GT.IDBZM) IDBZM=A(IY,IX)
      WRITE(IPRINT,7007) IDBZM
      ITEST=IDBZM/2
      ITEST1=ITEST*2
      IF(IDBZM-ITEST1) 408,408,409
408   ITSLD=IDBZM+2
      GO TO 410
409   ITSLD=IDBZM+1
410   CONTINUE
      WRITE(IPRINT,7001)
      DO 850 IRS=1,50
C     DETERMINE THE THRESHOLD VALUE AND MAKE SURE IT EXCEEDS 20 DBZ
      ITSLD=ITSLD-2
      NMAX=1
      IF(ITSLD.LT.20) GO TO 840
      GO TO 841
840   IRS=50
      GO TO 850
```

```
C       INITIALIZE THE POINTER ARRAYS IPB AND IPE AND THE SUM ARRAYS
841     DO 842 ID=1,IMAXR
        DO 842 IDD=1,300
        IPB(IDD,ID)=-999
        IPE(IDD,ID)=999
        SUMR(IDD)=0.0
        SUMZ(IDD)=0.0
842     SUMT(IDD)=0.0
C       INITIALIZE THE IBEG AND IEND ARRAYS
        DO 333 IBJ=1,IMAXR
        DO 333 IJB=1,20
        IBEG(IBJ,IJB)=999
333     IEND(IBJ,IJB)=-999
        DO 334 IFF=1,99
334     IMA(IFF)=0
C       NOW LOAD THE BEGINNING AND ENDING POINTS ON EACH AZIMUTH WHICH ARE
C       IN EXCESS OF THE THRESHOLD INTO IBEG AND IEND
        DO 10 IY=IYMIN,IYMAX
        K=1
        ISW=0
        IBEG(IY,1)=999
        IEND(IY,1)=-999
        DO 30 IX=1,IXMAX
        IF(A(IY,IX).LT.ITSLD) GO TO 20
        ISW=1
        IF(IX.LT.IBEG(IY,K)) IBEG(IY,K)=IX
        IF(IX.GT.IEND(IY,K)) IEND(IY,K)=IX
        GO TO 30
20      IF(ISW.EQ.1) K=K+1
        IBEG(IY,K)=999
        IEND(IY,K)=-999
        ISW=0
30      CONTINUE
        IF(ISW.EQ.0) K=K-1
        I(IY)=K
```

```
      K=1
10    CONTINUE
C     INITIALIZE THE DUMMY AZIMUTH
      IYB=IMAXR+1
      DO 993 IQ=1,300
      IPB(IQ,IYB)=-999
      IPE(IQ,IYB)=999
      IF(IQ.GT.100) GO TO 993
      A(IYB,IQ)=0
      IF(IQ.GT.20) GO TO 993
      IBEG(IYB,IQ)=999
      IEND(IYB,IQ)=-999
993   CONTINUE
      I(IYB)=1
      ICOUNT=-1
C     CYCLE THROUGH THE RAYS  CONSIDERING TWO CONSECUTIVE RAYS AT A TIME
C     CHECKING FOR CONTINUING AREAS IN EXCESS OF THRESHOLD
      IYE=IYMAX-1
      DO 190 II=IYMIN,IYMAX
      ICOUNT=ICOUNT+1
      KL=II+1
      NFL=I(II)
      KFL=I(KL)
      DO 120 KK=1,NFL
      DO 120 LL=1,KFL
      IF(IBEG(II,KK).GE.IBEG(KL,LL)) GO TO 300
      GO TO 600
300   IF(IBEG(II,KK).LE.(IEND(KL,LL)+1)) GO TO 200
      GO TO 120
600   IF((IEND(II,KK)+1).GE.IBEG(KL,LL)) GO TO 200
      GO TO 120
200   N=1
201   IF(IBEG(II,KK).GE.IPB(N,II).AND.IBEG(II,KK).LE.IPE(N,II))GO TO 400
      IF(IPB(N,KL)+999) 800,800,900
800   IPB(N,KL)=0
```

```
      IPE(N,KL)=0
900   IF(IBEG(II,KK).EQ.1) GO TO 901
      IF((IBEG(II,KK)-1).GE.IPB(N,KL).AND.(IBEG(II,KK)-1).LE.IPE(N,KL))G
     AO TO 400
      GO TO 902
901   IF(IBEG(II,KK).GE.IPB(N,KL).AND.IBEG(II,KK).LE.IPE(N,KL))GO TO 400
902   N=N+1
      IF(N.GT.NMAX) NMAX=N
      GO TO 201
C     WHEN MATCHES ARE FOUND COMPUTE THE NECESSARY SUMS AND LOAD INTO POINTER
C     ARRAYS THE BIN NUMBERS WHICH HAVE BEEN SUMMED
400   SUMD=0.0
      IF(IPB(N,II).LT.0)GO TO 81
      IF(IBEG(II,KK).GE.IPB(N,II).AND.IBEG(II,KK).LE.IPE(N,II)) GO TO 50
81    IDB=IBEG(II,KK)
      IDE=IEND(II,KK)
      DO 2 JJ=IDB,IDE
      SUMD=SUMD+AREA(JJ)
      SUMR(N)=SUMR(N)+RANGE(JJ)*AREA(JJ)
2     SUMZ(N)=SUMZ(N)+FLOAT(II)*AREA(JJ)
      IF(IPB(N,II).GT.0) GO TO 48
      IPB(N,II)=IBEG(II,KK)
48    IPE(N,II)=IEND(II,KK)
50    IF(IPB(N,KL).LT.0) GO TO 82
C     CHECK FOR OVERLAPPING TO PREVENT RESUMMING OF BINS
      DO 104 IIR=1,NMAX
      IF(IBEG(KL,LL).GE.IPB(IIR,KL).AND.IBEG(KL,LL).LE.IPE(IIR,KL)) GO
     BTO 61
      GO TO 104
61    IF(IPB(IIR,KL).LT.0) GO TO 104
      IVAR=IIR
      GO TO 51
104   CONTINUE
82    IVAR=N
      IFB=IBEG(KL,LL)
```

```
      IFE=IEND(KL,LL)
      DO 3 MM=IFB,IFE
      SUMD=SUMD+AREA(MM)
      SUMR(N)=SUMR(N)+RANGE(MM)*AREA(MM)
3     SUM7(N)=SUM7(N)+FLOAT(KL)*AREA(MM)
      IF(IPB(N,KL).GT.0) GO TO 49
      IPB(N,KL)=IBEG(KL,LL)
49    IPE(N,KL)=IEND(KL,LL)
51    SUMT(N)=SUMT(N)+SUMD
C     MERGE OVERLAPPING AREAS INTO ONE AREA
      IC=0
      DO 37 NN=1,NMAX
      IF(IBEG(KL,LL).NE.1) GO TO 18
      IB=1
      GO TO 19
18    IB=IBEG(KL,LL)-1
19    IF(IEND(KL,LL).NE.100) GO TO 22
      IE=100
      GO TO 21
22    IE=IEND(KL,LL)+1
21    CONTINUE
      DO 930 IN=IB,IE
      IF((IN.GE.IPB(NN,II)).AND.(IN.LE.IPE(NN,II))) GO TO 39
      GO TO 930
39    IC=IC+1
      IMA(IC)=NN
      GO TO 37
930   CONTINUE
37    CONTINUE
      IF(IC.GT.1) GO TO 38
      GO TO 120
38    LK=IMA(1)
      DO 41 IM=2,IC
      IS=IMA(IM)
      SUMR(LK)=SUMR(LK)+SUMR(IS)
```

```
      SUMZ(LK)=SUMZ(LK)+SUMZ(IS)
      SUMT(LK)=SUMT(LK)+SUMT(IS)
      SUMR(IS)=0.0
      SUMZ(IS)=0.0
41    SUMT(IS)=0.0
      IF(IVAR.EQ.LK) GO TO 55
      IPB(LK,KL)=IPB(IVAR,KL)
      IPB(IVAR,KL)=0
      IPE(LK,KL)=IPE(IVAR,KL)
      IPE(IVAR,KL)=0
55    IDM=999
      IDX=-999
      DO 42 IIM=1,IC
      IT=IMA(IIM)
      IF(IPB(IT,II).LT.IDM)IDM=IPB(IT,II)
      IPB(IT,II)=0
      IF(IPE(IT,II).GT.IDX)IDX=IPE(IT,II)
42    IPE(IT,II)=0
      IPB(LK,II)=IDM
      IPE(LK,II)=IDX
120   CONTINUE
130   IBR=I(II)
      DO 71 N2=1,IBR
      IF(IBEG(II,N2).EQ.0) GO TO 70
      IF((IBEG(II,N2)-999).EQ.0) GO TO 70
      GO TO 72
70    N2=IBR
      GO TO 71
72    NMA=NMAX
      DO 71 NGB=1,NMA
      IF(IBEG(II,N2).GE.IPB(NGB,II).AND.IBEG(II,N2).LE.IPE(NGB,II))GO TO
     A73
      IF(NGB.EQ.NMA) GO TO 74
      GO TO 71
73    IF(IPB(NGB,II).LT.0) GO TO 74
```

```
      NGB=NMA
      GO TO 71
74    NMAX=NMAX+1
      IL1=IBEG(II,N2)
      IL2=IEND(II,N2)
      DO 75 MST=IL1,IL2
      SUMR(NMAX)=SUMR(NMAX)+RANGE(MST)*AREA(MST)
      SUMZ(NMAX)=SUMZ(NMAX)+FLOAT(II)*AREA(MST)
75    SUMT(NMAX)=SUMT(NMAX)+AREA(MST)
      IPB(NMAX,II)=IL1
      IPE(NMAX,II)=IL2
      NGB=NMAX
71    CONTINUE
77    IF(ICOUNT.EQ.0) GO TO 190
      IF(II.GT.IYE) GO TO 190
      DO 60 IIJ=1,NMAX
      IF(IPB(IIJ,KL).GT.0)GO TO 60
      IPB(IIJ,KL+1)=0
      IPB(IIJ,KL)=0
      IPE(IIJ,KL+1)=0
      IPE(IIJ,KL)=0
60    CONTINUE
190   CONTINUE
C     OUTPUT THE THRESHOLD, AREA NUMBER, TOTAL AREAL COVERAGE,
C     AVERAGE RANGE AND AVERAGE AZIMUTH
C     ITOT IS THE AREA COUNTER,AREMA IS THE MAX AREA SIZE, AVERA IS THE
C     AVERAGE AREA SIZE, TOTAR IS THE TOTAL AREA COVERED
      ITOT=0
      AREMA=0.0
      TOTAR=0.0
      AVERA=0.0
737   DO 561 MN=1,NMAX
      IF(SUMT(MN).EQ.0.0) GO TO 561
      ITOT=ITOT+1
      TOTAR=TOTAR+SUMT(MN)
```

```
      IF(SUMT(MN).GT.AREMA) AREMA=SUMT(MN)
      AZB=SUMZ(MN)/SUMT(MN)
      INAZ=AZB
      REAZ=AZB-FLOAT(INAZ)
      IBAZ=AZAR(INAZ)
      REAZ=REAZ+FLOAT(IBAZ)
      ZF=SUMR(MN)/SUMT(MN)
      ROOT4=(SUMT(MN))**.25
      WRITE(IPRINT,7002) ITSLD,MN,SUMT(MN),ZF,REAZ,ROOT4
561   CONTINUE
      AVERA=TOTAR/FLOAT(ITOT)
      WRITE(IPRINT,7010) ITOT,TOTAR,AVERA,AREMA
850   CONTINUE
7001  FORMAT(15X,53HTHRESHOLD  AREA # TOTAL AREA  RBAR  AZBAR  AREA ROOT
     A4,/17X,51H(DBZ)              (NM**2)   (NM)  (DEG)    (NM**.50)/)
7002  FORMAT(18X,I2,8X,I3,3X,F9.4,2X,F5.1,1X,F5.1,3X,E9.4/)
7003  FORMAT(15X,5E20.5)
7004  FORMAT(15X,27HFOLLOWING IS THE AREA ARRAY,/)
7005  FORMAT(15X,64HRANGE(NM)      # GATES SKIPPED      RANGE STEP(NM)
     A AREA FACTOR)
7006  FORMAT(16X,F6.1,10X,I5,17X,F4.1,11X,F9.7)
7007  FORMAT(15X,8HMAX DBZ=,I5)
7008  FORMAT(1H ,I4,3X,40I3)
7009  FORMAT(1H ,I4,3X,25I3)
7010  FORMAT(5X,9HTHERE ARE,I4,16H AREAS COVERING ,E9.4,29H SQ NM.  THE
     AAVERAGE SIZE IS ,E9.4,20H AND THE MAXIMUM IS ,E9.4,7H SQ NM.)
1001  FORMAT(3I5,F6.1)
1002  FORMAT(I3)
1003  FORMAT(20I3)
      STOP
      END
```